

# Estimation of positive definite $M$ -matrices and structure learning for attractive Gaussian Markov Random fields

Martin Slawski and Matthias Hein

{ms,hein}@cs.uni-saarland.de

Saarland University

Department of Computer Science, Campus E 1.1, 66041 Saarbrücken

---

## Abstract

Consider a random vector with finite second moments. If its precision matrix is an  $M$ -matrix, then all partial correlations are non-negative. If that random vector is additionally Gaussian, the corresponding Markov random field (GMRF) is called *attractive*.

We study estimation of  $M$ -matrices taking the role of inverse second moment or precision matrices using sign-constrained log-determinant divergence minimization. We also treat the high-dimensional case with the number of variables exceeding the sample size. The additional sign-constraints turn out to greatly simplify the estimation problem: we provide evidence that explicit regularization is no longer required. To solve the resulting convex optimization problem, we propose an algorithm based on block coordinate descent, in which each sub-problem can be recast as non-negative least squares problem. Illustrations on both simulated and real world data are provided.

*Keywords:*  $\ell_1$ -regularization, log-determinant divergence minimization, Gaussian Markov Random Fields, Graphical Model Selection, high-dimensional statistical inference,  $M$ -matrices, partial correlations, precision matrix estimation, sign constraints

*2010 MSC:* 62H12, 62F30, 15B35, 90C25

---

## 1. Introduction

The covariance matrix of a random vector and its inverse play an important role in multivariate statistical analysis due to their presence, for example, in PCA, discriminant analysis, tests of hypotheses and confidence

intervals for the mean. The sparsity pattern of the inverse covariance, or synonymously precision matrix, reveals all pairwise conditional independence relations in a Gaussian Markov random field (GMRF), which correspond to missing edges in the resulting conditional independence graph [53, 33, 45]. The latter is central to Gaussian graphical modelling [15], where one aims at a parameter-parsimonious models in terms of a conditional independence graph consisting of few edges. In recent years, precision matrix estimation and Gaussian graphical models (GGMs) have received considerable attention in statistics, machine learning and optimization due to the prevalence of high-dimensional datasets in areas such as genomics, finance and neuroscience for which the number of variables  $p$  is comparable or even larger than the sample size  $n$ . This setup has stimulated the development of various new inferential procedures typically hinging on sparsity assumptions on the precision matrix. One class of approaches tries to infer only its sparsity pattern, or equivalently in the multivariate Gaussian case, the edges of the conditional independence graph. For this purpose, procedures based on conditional independence tests [27, 2] and nodewise sparse regression (*neighbourhood selection* [38, 56]) have been suggested. Given the graph structure, the precision matrix can be estimated subject to additional constraints [11, 14]. A second line of research is concerned with estimation of the precision matrix with the help of sparsity-promoting regularization schemes. In the references [55, 3, 22, 44, 21, 42]  $\ell_1$ -regularized log-determinant divergence minimization, which amounts to  $\ell_1$ -penalized maximum likelihood estimation in the Gaussian case, is investigated. Related regularization schemes enforcing sparsity of the off-diagonal elements of the precision matrix are proposed in [20, 54, 9, 47]. In [18] and [25], regularization schemes to enforce different forms of structured sparsity are considered. In the present paper, we adopt the high-dimensional setting that is addressed in the cited references, while considering elements from a subcone of the positive semidefinite cone as target in precision matrix estimation. Specifically, we consider positive definite matrices that are symmetric  $M$ -matrices [40, 4], i.e. elements of the set

$$\mathcal{M}^p = \{\Omega = (\omega_{jk}) \in \mathbb{R}^{p \times p} : \Omega \in \mathbb{S}_+^p, \omega_{jk} \leq 0, j, k = 1, \dots, p, j \neq k\}, \quad (1)$$

where  $\mathbb{S}_+^p = \{\Omega \in \mathbb{R}^{p \times p} : \Omega = \Omega^\top, \Omega \succ 0\}$  denotes the set of symmetric, positive definite matrices. In the statistics literature, Bølviken [19] appears to be the first to consider matrices (1) as precision matrices whose partial correlations  $-\omega_{jk}/\{\omega_{jj}\omega_{kk}\}^{1/2}$ ,  $j \neq k$ , are all non-negative. Karlin and Rinott

[30] studied elements from (1) as covariance or precision matrices of a multivariate Gaussian distribution with a focus on total positivity [29]; see also [43]. In [35, 2], the GMRF corresponding to a precision matrix of the form (1) is referred to as *attractive* GMRF. In [35], attractive GMRFs are shown to be a sub-class of *non-frustrated* GMRFs, which in turn form a sub-class of *walk-summable* GMRFs. Statistical inference specifically for the class (1), has, to the best of our knowledge, not been studied in the literature. In [32], the authors consider MAP estimation for the case that the precision matrix of a Gaussian random vector belongs to the following subset of (1):

$$\mathcal{L}_I^p = \left\{ \Omega \in \mathbb{R}^{p \times p} : \Omega = \kappa I - W + \text{diag} \left( \sum_{k=1}^p w_{1p}, \dots, \sum_{k=1}^p w_{pk} \right), \right. \\ \left. \kappa > 0, w_{jk} = w_{kj}, w_{jk} \geq 0, j, k = 1, \dots, p, j \neq k \right\} \subset \mathcal{M}^p, \quad (2)$$

where the containment in  $\mathcal{M}^p$  holds because by construction, all elements of  $\mathcal{L}_I^p$  are diagonally dominant and thus positive definite. We note that (2) equals the set of matrices that can be written as a positive multiple of the identity plus the combinatorial Laplacian of an undirected graph on  $p$  vertices and positive edge weights  $w_{jk}$ ,  $j, k = 1, \dots, p$ . In [32], an exponential prior for the weights is proposed, so that MAP estimation amounts to  $\ell_1$ -penalized maximum likelihood estimation. As discussed in more detail below, restricting the class of admissible precision matrices by imposing sign-constraints on the off-diagonals as in (1) and (2) can be a blessing and a curse at the same time. On the negative side, the requirement that all partial non-negative correlations be non-negative is realistically not fulfilled in most contemporary datasets. For example, in gene expression analysis, genes may have both up- and down-regulatory effects on other genes. It is a priori unclear what the consequences of estimation under model misspecification are (see Section 2.3 below). On the positive side, we show that the presence of the additional sign constraints suffices to establish existence and uniqueness of maximum likelihood estimation in the Gaussian case even in a high-dimensional regime ( $n < p$ ), which is unlike the unconstrained case. Furthermore, we present empirical evidence that explicit regularization is not required and that subsequent thresholding of the off-diagonal entries of the constrained estimate yields a simple yet effective procedure to recover the sparsity pattern of an underlying sparse target from the class (1) and hence also the structure

of the associated graph. This is akin to recent work on (thresholded) non-negative least squares in high-dimensional sparse regression [49, 37]. Absence of tuning parameters and the tendency to produce sparse solutions make the approach attractive in exploratory data analysis when the goal is to find a sparse graph depicting positive dependence relations among variables. In [32], learning taxonomies is presented as an example where only positive dependence are of interest. In the present paper, we also discuss a possible application to the analysis of landmark data similar in spirit to [24].

*Outline.* In Section 2, we study central properties of sign-constrained log-determinant divergence minimization and positive definite  $M$ -matrices. Sparse estimation based on thresholding is subsequently discussed in Section 3. In Section 4, we develop a block coordinate descent algorithm to solve the resulting convex optimization problem and prove its convergence. An extensive empirical study including the analysis of real world datasets is presented in Section 5. We conclude with a short summary. The appendix contains all proofs.

*Notation.* Matrices are denoted by uppercase Latin or Greek letters and its elements by the corresponding lowercase letters. For matrices starting with the letter  $\Omega$ , the letter  $\Sigma$  is used for their inverses. We use double subscripts to denote submatrices, i.e.  $A_{IJ}$  is the submatrix of some matrix  $A$  with row indices  $I$  and column indices  $J$ . We write  $A_{II}^{-1} = (A_{II})^{-1}$  for the inverse of a square invertible sub-matrix  $A_{II}$  of  $A$ . A superscript  $c$  denotes the set complement. We will frequently arrange a symmetric and invertible matrix  $A \in \mathbb{R}^{p \times p}$  in the following way. For  $j \in \{1, \dots, p\}$  arbitrary, let  $a_j \in \mathbb{R}^{p-1}$  be the vector with components  $a_{jk}$ ,  $k = 1, \dots, p$ ,  $k \neq j$ , and  $A_{jj} \in \mathbb{R}^{(p-1) \times (p-1)}$  the square submatrix of  $A$  having entries  $\{a_{lm}, l, m \neq j\}$ . After row and column permutations,  $A$  and accordingly its inverse  $B$  can be partitioned as

$$\begin{bmatrix} a_{jj} & a_j^\top \\ a_j & A_{jj} \end{bmatrix}, \quad \text{respectively} \quad \begin{bmatrix} b_{jj} & b_j^\top \\ b_j & B_{jj} \end{bmatrix}, \quad (3)$$

where  $b_{jj}$ ,  $B_{jj}$  and  $b_j$  are given by

$$b_{jj} = \frac{1}{a_{jj} - a_j^\top A_{jj}^{-1} a_j}, \quad B_{jj} = \left( A_{jj} - \frac{a_j a_j^\top}{a_{jj}} \right)^{-1}, \quad b_j = -b_{jj} \cdot A_{jj}^{-1} a_j. \quad (4)$$

For a square matrix  $A$ ,  $D(A)$  denotes the matrix resulting from  $A$  after setting all off-diagonal entries to zero. Likewise,  $\text{off}(A)$  denotes the matrix

resulting from  $A$  after setting all diagonal elements to zero. Moreover,  $\text{tr}(A)$  denotes the trace of  $A$ . For square matrices  $A_1, \dots, A_K$ ,  $\text{bdiag}(A_1, \dots, A_K)$  denotes the block diagonal matrix composed of these matrices. We write  $A \succ 0$  and  $A \succeq 0$  for a positive definite respectively positive semidefinite matrix  $A$ , whereas  $\leq, \geq, <, >$  are used to denote component-wise inequalities, e.g.  $A \leq B$  means that  $a_{jk} \leq b_{jk}$  for all  $j$  and  $k$ . The symbols  $I$  and  $\mathbf{1}$  are used to denote identity matrices and vectors of ones, respectively.

## 2. Positive definite $M$ -matrices and sign-constrained log-determinant divergence minimization

### 2.1. Problem formulation

Let  $x_1, \dots, x_n$  be a sample of  $n$  i.i.d. realizations from a multivariate Gaussian random vector  $X$  with mean  $\mu_* \in \mathbb{R}^p$  and covariance  $\Sigma_* = (\sigma_{jk}^*) \in \mathbb{S}_+^p$  and precision matrix  $\Sigma_*^{-1} = \Omega_* = (\omega_{jk}^*)$ . Assuming that  $\mu_*$  is known and that  $\Omega_* \in \mathcal{M}^p$  as defined in (1), constrained maximum likelihood estimation of  $\Omega_*$  leads to the minimization problem

$$\min_{\Omega \in \mathcal{M}^p} -\log \det(\Omega) + \text{tr}(\Omega S), \quad \text{where } S = \frac{1}{n} \sum_{i=1}^n (x_i - \mu_*)(x_i - \mu_*)^\top. \quad (5)$$

In case that  $\Omega_* \notin \mathcal{M}^p$  or  $X$  is non-Gaussian, (5) can be understood as  $M$ -estimation based on minimizing the Bregman divergence between positive definite matrices that is induced by the function  $\Omega \mapsto -\log \det(\Omega)$ , cf. [16, 42] and (14) below. Accordingly, we will henceforth refer to (5) and related problems as (constrained or regularized) log-determinant divergence minimization. It is well known that if  $\mathcal{M}^p$  in (5) is replaced by  $\mathbb{S}_+^p$ , i.e. if the additional sign-constraints on the off-diagonal elements are omitted, and  $p > n$ , a minimizer of (5) in general does not exist since the minimum in (5) is not finite. Hence, it is a priori unclear whether the minimization problem (5) is well-defined in the case  $p > n$ . As stated in the following theorem, the additional constraint  $\Omega \in \mathcal{M}^p$  makes a drastic difference.

**Theorem 1.** *Consider the optimization problem (5) and suppose that  $S = (s_{jk})$  has strictly positive diagonal elements. Then, unless there exists  $(j, k), j \neq k$ , such that  $s_{jk} = \sqrt{s_{jj}s_{kk}}$ , a minimizer of (5) exists and is unique.*

In other words, unless there exists a pair of variables of perfect positive sample correlation, which can easily be checked in practice, the constrained log-determinant divergence minimization problem (5) is well-posed,

even though one may have  $n < p$  and no additional regularization is employed. We note that the conditions of Theorem 1 are mild, because they are fulfilled with probability one provided  $n > 1$  and the random vector  $X$  has a distribution that is absolutely continuous w.r.t. the Lebesgue measure.

## 2.2. Optimality conditions and dual problem

Within the present subsection, we study problem (5) from the point of view of convex optimization. It is standard to extend the negative log-determinant to the entire positive semidefinite cone  $\overline{\mathbb{S}}_+^p = \{\Omega \in \mathbb{R}^{p \times p} : \Omega = \Omega^\top, \Omega \succeq 0\}$  by setting  $-\log \det(\Omega) = +\infty$  if  $\Omega \notin \mathbb{S}_+^p$ . Accordingly, we define  $\overline{\mathcal{M}}^p$  as the subset of matrices in  $\overline{\mathbb{S}}_+^p$  having only non-positive off-diagonal elements. We may then re-write (5) as

$$\min_{\Omega \in \overline{\mathcal{M}}^p} -\log \det(\Omega) + \text{tr}(\Omega S), \quad (6)$$

which constitutes a convex optimization problem. In fact, the constraint set, as the intersection of two convex cones, is a convex cone, and the negative log-determinant is convex on  $\overline{\mathbb{S}}_+^p$ , cf. [7]. The Lagrangian for (6) is given by

$$L(\Omega, \Gamma) = -\log \det(\Omega) + \text{tr}(\Omega S) + \text{tr}(\Omega \Gamma), \quad (7)$$

where  $\Gamma = (\gamma_{jk})$  is a symmetric, non-negative matrix of Lagrangian multipliers with all diagonal entries being zero. By the Karush-Kuhn-Tucker (KKT) optimality conditions,  $(\widehat{\Omega}, \widehat{\Gamma})$  is an optimal solution if and only if

$$S + \widehat{\Gamma} = \widehat{\Omega}^{-1}, \quad \text{tr}(\widehat{\Omega} \widehat{\Gamma}) = 0, \quad \widehat{\Omega} \in \overline{\mathcal{M}}^p, \quad \widehat{\Gamma} \in \mathbb{R}_+^{p \times p}, \quad \widehat{\Gamma} = \widehat{\Gamma}^\top, \quad \text{diag}(\widehat{\Gamma}) = 0. \quad (8)$$

Note that under the stated conditions

$$\text{tr}(\widehat{\Omega} \widehat{\Gamma}) = 0 \iff \widehat{\omega}_{jk} \widehat{\gamma}_{jk} = 0, \quad j, k = 1, \dots, p. \quad (9)$$

Convex duality yields

$$\begin{aligned} \min_{\Omega \in \overline{\mathcal{M}}^p} -\log \det(\Omega) + \text{tr}(\Omega S) &= \max_{\Gamma \geq 0, \text{diag}(\Gamma)=0} \min_{\Omega \in \overline{\mathcal{M}}^p} L(\Omega, \Gamma) \\ &= \max_{S+\Gamma \in \overline{\mathbb{S}}_+^p, \Gamma \geq 0, \text{diag}(\Gamma)=0} \log \det(S + \Gamma) + p \\ &= \max_{\Sigma \in \overline{\mathbb{S}}_+^p, \Sigma \geq S, \text{diag}(\Sigma)=\text{diag}(S)} \log \det(\Sigma) + p. \end{aligned} \quad (10)$$

The second identity follows after taking the derivative of  $L$  w.r.t.  $\Omega$ , setting the result to zero and substituting this relation back into  $L$  (cf. the first condition in (8)), while the third equality is by a change of variables. In other words, in the problem dual to (7), one seeks for a positive definite matrix of maximum determinant, which dominates  $S$  entry-wise and has the same diagonal entries. As corollary, we obtain the following characterization of *inverse* positive definite  $M$ -matrices.

**Theorem 2.**  $\Sigma \in \mathbb{S}_+^p$  is an inverse  $M$ -matrix if and only if

$$\operatorname{argmax}_{\Sigma' \in \overline{\mathbb{S}_+^p}, \Sigma' \geq \Sigma, \operatorname{diag}(\Sigma') = \operatorname{diag}(\Sigma)} \log \det(\Sigma') = \Sigma.$$

From (10), we can also read off necessity of the condition in Theorem 1: if there is a pair of variables of perfect positive sample correlation, it is not possible to find  $\Sigma \geq S$  with  $\operatorname{diag}(\Sigma) = \operatorname{diag}(S)$  that is strictly positive definite, so that (10) is unbounded from below.

### 2.3. The class $\mathcal{M}^p$ as a model of multivariate dependence: restrictions and consequences of mis-specification

Recapitulating facts from [4, 30], we will see that the constraint  $\Omega \in \mathcal{M}^p$  induces a rather specific model of multivariate dependence for an underlying random vector  $X = (X_j)_{j=1}^p$ . Consequently, the target  $\Omega_*$  can in general not be expected to satisfy the given constraint. It is therefore of interest to know how sign-constrained log-determinant divergence minimization (6) behaves under model mis-specification, and we will investigate this issue for selected examples.

*M-matrices as precision matrices.* Let  $\Omega \in \mathcal{M}^p$ . Then, it is not hard to see that  $\Omega = \delta I - B$  for symmetric  $B \in \mathbb{R}_+^{p \times p}$  and  $\delta \in (\lambda_1(B), \infty)$ , where  $\lambda_1$  denotes the largest eigenvalue of  $B$  (cf. Appendix A). Expressing the inverse by a Neumann series, one obtains  $\Sigma = \Omega^{-1} = \delta^{-1} \sum_{k=0}^{\infty} (B/\delta)^k$  and hence  $\Sigma \in \mathbb{R}_+^{p \times p}$ . That is, a precision matrix with non-positive off-diagonal entries implies non-negative marginal correlations, i.e.  $\operatorname{Cov}(X_j, X_k) \geq 0$  for all  $j, k$ . More generally, for any pair of variables  $(X_j, X_k)$  and any set of conditioning variables  $(X_l)_{l \in L}$ ,  $L \subseteq \{1, \dots, p\} \setminus \{j, k\}$ , the partial correlation of  $(X_j, X_k)$  conditional on  $X_L$  is non-negative. This follows from the fact that covariances conditional on  $L$  are given by the Schur complement of  $\Sigma$  w.r.t.  $L$ , that is

$$\Sigma_{L^c L^c} - \Sigma_{L^c L} \Sigma_{LL}^{-1} \Sigma_{LL^c} = \Omega_{L^c L^c}^{-1}, \quad (11)$$

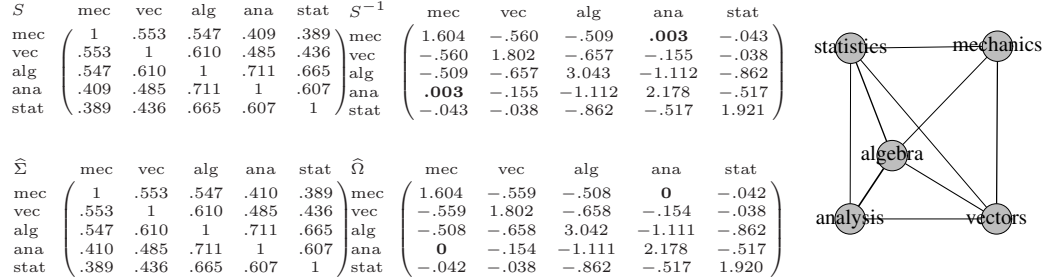


Figure 1: Solution pair  $(\widehat{\Sigma}, \widehat{\Omega})$  for the math marks dataset with correlation matrix  $S$ . The edge widths of the graph correspond to partial correlations inferred from  $\widehat{\Omega}$ .

where the right hand side results by using partitioned inverses. Since  $\Omega$  is an  $M$ -matrix, so must be the sub-matrix  $\Omega_{L^c L^c}$  and the claim follows from the same argument as above. Exchanging roles of  $\Sigma$  and  $\Omega$  in (11), we find that

$$\Omega_{L^c L^c} - \Omega_{L^c L} \Omega_{LL}^{-1} \Omega_{LL^c} = \Sigma_{L^c L^c}^{-1}, \quad (12)$$

the Schur complement of  $\Omega$  w.r.t.  $L$ , is an  $M$ -matrix, or equivalently, that the principal sub-matrix  $\Sigma_{L^c L^c}$  of  $\Sigma$  is an inverse  $M$ -matrix. This observation implies that the sign of the partial correlations remain unchanged when confining oneself to any subset of variables. To verify this, note that  $\Omega_{LL} \in \mathcal{M}^{|L|}$  implies that  $\Omega_{LL}^{-1} \geq 0$ . Combining this with  $\Omega_{L^c L} \leq 0$ , we have that  $\Omega_{L^c L} \Omega_{LL}^{-1} \Omega_{LL^c} \geq 0$ , and in turn that the off-diagonal entries of the Schur complement are non-positive.

Finally, we remark that the regression coefficients of a linear regression for any variable  $X_j$  on the remaining variables are non-negative. To see this, first partition  $\Sigma$  and  $\Omega$  as in (3):

$$\begin{bmatrix} \sigma_{jj} & \sigma_j^\top \\ \sigma_j & \Sigma_{jj} \end{bmatrix}, \quad \text{and} \quad \begin{bmatrix} \omega_{jj} & \omega_j^\top \\ \omega_j & \Omega_{jj} \end{bmatrix}.$$

The regression coefficients equal  $\Sigma_{jj}^{-1} \sigma_j = -\omega_j / \omega_{jj} \in \mathbb{R}_+^{p-1}$  in view of (4), which are non-negative as  $\Omega$  has only non-positive off-diagonal elements.

*Example: Math marks data.* The math marks dataset [36, 53] contains the marks of  $n = 88$  students achieved in  $p = 5$  subjects of mathematics ('mechanics', 'vectors', 'algebra', 'analysis', 'statistics'). Figure 1 shows the resulting sample correlation matrix, its inverse and the solution pair  $(\widehat{\Sigma}, \widehat{\Omega})$



of the minimization problem (6) obtained with the computational approach described in Section 4 below. The  $M$ -matrix model for the precision matrix appears to be adequate, with  $(\widehat{\Sigma}, \widehat{\Omega})$  closely matching  $(S, S^{-1})$ . There is only one pair of variables that yields a tiny positive off-diagonal entry in  $S^{-1}$ , which equals exactly zero in  $\widehat{\Omega}$ . From a practical point of view, the good fit of the  $M$ -matrix model suggests that if a student's performance in a subset of disciplines increase, then so does the performance the remaining disciplines, i.e. it least remains constant, but there is no drop in performance.

*Model mis-specification.* Since the constraint  $\Omega \in \mathcal{M}^p$  is rather strong, it is important to have some understanding about how sign-constrained log-determinant divergence minimization (6) behaves under mis-specification, i.e. the population precision matrix  $\Omega_* \notin \mathcal{M}^p$ . In this case, the estimator  $\widehat{\Omega}$  may be subject to a substantial bias. In the following, we discuss this issue at the population level. To this end, we define

$$\Omega_{\bullet} = \operatorname{argmin}_{\Omega \in \overline{\mathcal{M}^p}} -\log \det(\Omega) + \operatorname{tr}(\Omega \Sigma_*) \quad (13)$$

$$\begin{aligned} &= \operatorname{argmin}_{\Omega \in \overline{\mathcal{M}^p}} -\log \det(\Omega) + \log \det(\Omega_*) + \operatorname{tr}((\Omega - \Omega_*) \Sigma_*) \\ &=: \operatorname{argmin}_{\Omega \in \overline{\mathcal{M}^p}} D(\Omega_* \parallel \Omega), \end{aligned} \quad (14)$$

where  $D(\Omega_* \parallel \Omega)$  denotes the Bregman divergence of  $\Omega$  from  $\Omega_*$ , which coincides (apart from a factor of 1/2) with the Kullback-Leibler divergence of two zero-mean Gaussian distributions with precision matrices  $\Omega$  and  $\Omega_*$ , respectively. Note that according to the dual problem (10),  $\Sigma_{\bullet} = \Omega_{\bullet}^{-1}$  satisfies

$$\Sigma_{\bullet} = \operatorname{argmax}_{\Sigma \in \overline{\mathbb{S}_+^p}, \Sigma \geq \Sigma_*, \operatorname{diag}(\Sigma) = \operatorname{diag}(\Sigma_*)} \log \det(\Sigma). \quad (15)$$

Depending on the degree of mis-specification, it may be possible that  $\Omega_{\bullet}$  preserves positive partial correlations in  $\Omega_*$ . Ideally, one has for all  $j \neq k$

$$\omega_{jk}^{\bullet} = \omega_{jk}^* \quad \text{if } \omega_{jk}^* < 0, \quad \text{and } \omega_{jk}^{\bullet} = 0 \quad \text{otherwise.} \quad (16)$$

That is, entries matching the sign constraints are maintained, while negative partial correlations are zeroed out. If interest is only in the identification of pairs of variables of positive partial correlation and if (16) holds, then moving from  $\Omega_*$  to  $\Omega_{\bullet}$  does not result in a loss of information. For example,

in recommender systems, one is interested in finding pairs of items where the purchase of one item increases the chances of purchasing the other one. Several more examples are presented in Section 5. Beyond the ideal case (16), one can ask whether  $\Omega_\bullet$  at least preserves the pairs of negative sign, i.e. whether it holds that

$$\mathcal{E}^* = \{(j, k) : \omega_{jk}^* < 0\} = \mathcal{E}^\bullet = \{(j, k) : \omega_{jk}^\bullet < 0\}. \quad (17)$$

Below, we shed some light on this question for specific choices of  $(\Omega_*, \Sigma_*)$  for which it is possible to compute the corresponding solution pair  $(\Omega_\bullet, \Sigma_\bullet)$  in closed form.

(1) *Block structure.* Let  $\Omega_* \in \mathbb{S}_+^p$  be partitioned as

$$\Omega_* = \begin{bmatrix} \Omega_{*,11} & \Omega_{*,12} \\ \Omega_{*,21} & \Omega_{*,22} \end{bmatrix}, \quad \Omega_{*,11} \in \mathbb{S}_+^{p_1}, \quad \Omega_{*,22} \in \mathbb{S}_+^{p_2}, \quad \Omega_{*,12} = \Omega_{*,21}^\top \in \mathbb{R}^{p_2 \times p_1},$$

and let  $\Sigma_{*,11}$  etc. be defined accordingly.

(a). If  $\Omega_{*,11} \in \mathcal{M}^{p_1}$ ,  $\Sigma_{*,22} \in \mathcal{M}^{p_2}$  and  $\Omega_{*,12} = 0$ , then  $\Omega_\bullet$  in (13) is given by  $\Omega_\bullet = \text{bdiag}(\Omega_{*,11}, \{D(\Sigma_{*,22})\}^{-1})$ , where  $D(\Sigma_{*,22})$  is the restriction of  $\Sigma_{*,22}$  to its diagonal. In order to verify this, let us consider the dual in (15). We have  $\det(\Sigma_*) = \det(\Sigma_{*,11}) \cdot \det(\Sigma_{*,22}) \leq \det(\Sigma_{*,11}) \det(D(\Sigma_{*,22}))$  by Hadamard's inequality. Since we have  $D(\Sigma_{*,22}) \geq \Sigma_{*,22} \in \mathcal{M}^{p_2}$ ,  $\Sigma_\bullet = \text{bdiag}(\Sigma_{*,11}, D(\Sigma_{*,22}))$  is dual feasible. Given the upper bound on  $\det(\Sigma_*)$  and Theorem 2, it must be the solution (15). Observe that  $\Omega_\bullet$  fulfills (16).

(b). Let now  $\Omega_{*,11} \in \mathcal{M}^{p_1}$ ,  $\Omega_{*,22} \in \mathcal{M}^{p_2}$ ,  $\Omega_{*,12} \geq 0$ . Then we have  $\Omega_\bullet = \text{bdiag}(\Sigma_{*,11}^{-1}, \Sigma_{*,22}^{-1})$ . To see this, note that the partitioned inverse formula yields

$$\Sigma_{*,12} = -\Omega_{*,11}^{-1} \Omega_{*,12} (\Omega_{*,22} - \Omega_{*,21} \Omega_{*,11}^{-1} \Omega_{*,12})^{-1} = -\Omega_{*,11}^{-1} \Omega_{*,12} \Sigma_{*,22} \leq 0,$$

because  $\Omega_{*,11}^{-1}$ ,  $\Sigma_{*,22}$  and  $\Omega_{*,12}$  have only non-negative entries. Consequently,  $\Sigma_\bullet = \Omega_\bullet^{-1}$  is feasible for the dual in (15). Feasibility of  $\Omega_\bullet$  for the primal in (15) follows from

$$\text{off}(\Sigma_{*,11}^{-1}) = \text{off}(\Omega_{*,11} - \Omega_{*,12} \Omega_{*,22}^{-1} \Omega_{*,21}) \leq 0$$

and an according argument for  $\text{off}(\Sigma_{*,22}^{-1})$ . From the Hadamard-Fischer inequality, we obtain that  $\det(\Sigma_*) \leq \det(\Sigma_{*,11}) \cdot \det(\Sigma_{*,22})$ , and the claim follows from Theorem 2. Observe that  $\Omega_\bullet$  preserves signs according to (17).

The next two examples deal with precision matrices corresponding to stationary autoregressive (AR) processes of orders 1 and 2.

(2) *AR(1)-structure.* Let  $\Sigma_*$  have entries  $\sigma_{jk}^* = \rho^{|j-k|}$ ,  $j, k = 1, \dots, p$  for  $p$  even and  $-1 < \rho < 0$ . Then  $\sigma_{jk}^* < 0$  if one of  $(j, k)$  is even and the other one is odd, and  $\sigma_{jk}^* > 0$  if both of  $(j, k)$  are even/odd. The inverse  $\Omega_*$  is a band matrix of bandwidth one, the non-zero off-diagonal entries being all equal to  $-\rho/(1-\rho^2)$  (see e.g. [45], p.2). Set  $\Sigma_\bullet = \Sigma_* + \Gamma_\bullet$ , where the entries of  $\Gamma_\bullet$  are given by  $\gamma_{jk}^\bullet = 0$  if  $(j, k)$  are both even/odd and  $\gamma_{jk}^\bullet = -\sigma_{jk}^*$  otherwise. We will show that  $\Sigma_\bullet$  and its inverse  $\Omega_\bullet$  are the solutions (13)/(15) by verifying the KKT optimality conditions as given in (8). First note that  $\Sigma_\bullet \geq \Sigma_*$  and  $\Sigma_\bullet \in \mathbb{S}_+^p$ , where second claim can be seen from  $\Pi \Sigma_\bullet \Pi^\top = \text{bdiag}(\tilde{\Sigma}, \tilde{\Sigma})$ , where  $\Pi$  is a permutation matrix permuting odd rows  $1, 3, 5, \dots$  on the first  $1, \dots, p/2$  rows and the even rows on the rows  $p/2 + 1, p/2 + 2, \dots, p$ , and  $\tilde{\Sigma} \in \mathbb{R}^{p/2 \times p/2}$  has entries  $\tilde{\sigma}_{lm} = \rho^{2|l-m|} =: \phi^{|l-m|}$ ,  $l, m = 1, \dots, p/2$ , i.e.  $\tilde{\Sigma}$  has AR(1)-structure with parameter  $0 < \phi < 1$ . The non-zero off-diagonal entries of  $\tilde{\Sigma}^{-1}$  are all equal to  $-\phi/(1-\phi^2)$ , hence  $\Omega_\bullet \in \mathcal{M}^p$ . Finally observe that  $\Omega_\bullet$  satisfies the complementarity slackness condition  $\text{tr}(\Omega_\bullet \Gamma_\bullet) = 0$ .

Note that (17) is violated.

(3) *AR(2)-structure.* Let  $\Sigma_*$  have entries  $\sigma_{jk}^* = \rho_{|j-k|}$ , where  $\rho_\ell$ ,  $\ell = 1, \dots, p-1$ , is defined by the recursion

$$\rho_0 = 1, \quad \rho_1 = \frac{\phi_1}{1 - \phi_2}, \quad \rho_\ell = \phi_1 \rho_{\ell-1} + \phi_2 \rho_{\ell-2}, \quad \ell \geq 2. \quad (18)$$

for parameters  $\phi_1$  and  $\phi_2$  satisfying the stationarity condition

$$\left| \frac{1}{2\phi_2} \left( -\phi_1 + \sqrt{\phi_1^2 + 4\phi_2} \right) \right| > 1, \quad \left| \frac{1}{2\phi_2} \left( -\phi_1 - \sqrt{\phi_1^2 + 4\phi_2} \right) \right| > 1,$$

cf. [10]. The inverse  $\Omega_*$  has bandwidth two [45]. In the appendix, we prove that if  $4|\phi_2| < \phi_1$ , the minimizer  $\Omega_\bullet$  in (13) preserves signs according to (17). The condition  $4|\phi_2| < \phi_1$  is found to be tight in the sense that if it fails, (17) in general does not hold.

(4) *Star structure.* Let  $\Sigma_* = \begin{pmatrix} 1 & -\rho^\top \\ -\rho & I + \rho\rho^\top \end{pmatrix}$ , where  $\rho \in \mathbb{R}^{p-1}$ . The inverse results as  $\Omega_* = \begin{pmatrix} 1 + \|\rho\|_2^2 & \rho^\top \\ \rho & I \end{pmatrix}$ . In the appendix, it is shown that the

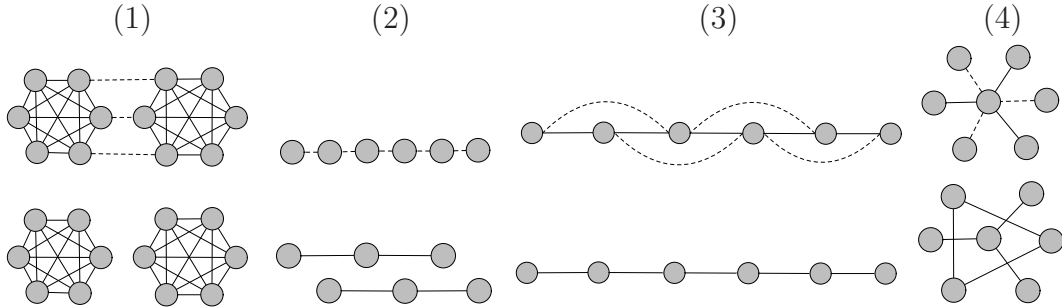


Figure 2: Graph-based description of the examples (1) to (4). Dashed edges correspond to positive off-diagonal entries and solid edges to negative ones. Top: graph structure of  $\Omega_*$ . Bottom: graph structure of  $\Omega_\bullet$ .

solutions (13)/(15) are given by

$$\Omega_\bullet = \begin{pmatrix} 1 + \|\tilde{\rho}\|_2^2 & \tilde{\rho}^\top \\ \tilde{\rho} & I - \frac{(\rho - \tilde{\rho})(\rho - \tilde{\rho})^\top}{1 + \|\rho - \tilde{\rho}\|_2^2} \end{pmatrix}, \quad \Sigma_\bullet = \begin{pmatrix} 1 & -\tilde{\rho}^\top \\ -\tilde{\rho} & I + \rho\rho^\top - \rho\tilde{\rho}^\top - \tilde{\rho}\rho^\top + 2\tilde{\rho}\tilde{\rho}^\top \end{pmatrix},$$

where  $\tilde{\rho} = (\min(\rho_j, 0))$ .

It follows that in general, sign preservation (17) does not hold: if  $\rho$  has at least two positive components  $j, k$ ,  $j \neq k$ , then  $\rho_j - \tilde{\rho}_j > 0$ ,  $\rho_k - \tilde{\rho}_k > 0$  and hence  $(\rho_j - \tilde{\rho}_j)(\rho_k - \tilde{\rho}_k) > 0$ , i.e. the corresponding entry in the bottom right block of  $\Omega_\bullet$  is negative.

Figure 2 provides a graphical description of the above four settings. In summary, it is not guaranteed that  $\Omega_\bullet$  recovers the set  $\mathcal{E}^*$  (17). While there are instances of  $\Omega_*$  where this is fulfilled, there are cases like the AR(1) example for which  $\Omega_\bullet$  even satisfies an opposite sign constraint. It is important to bear in mind that for simplicity, we have limited our discussion to the population setting. For a complete treatment, one would need to additionally take into account the effect resulting from the replacement of  $\Sigma_*$  by the sample covariance  $S$ .

### 3. Sparsification

Sparsity has been connected to precision matrix estimation since the seminal work of Dempster [15] on covariance selection. With the advent of high-dimensional data analysis, sparsity has become a key concept both to obtain

interpretable results and to establish guarantees of various concrete sparsity-promoting estimation techniques. Among these, penalty-based approaches are most prominent [3, 44, 20]. It hence appears natural to complement sign-constrained log-determinant divergence minimization (6) by such a penalty when sparsity is desired. This prompts the following modification of (6).

$$\min_{\Omega \in \overline{\mathcal{M}^p}} -\log \det(\Omega) + \text{tr}(\Omega S) + \lambda \sum_{(j,k):j \neq k} \text{pen}(\omega_{jk}), \quad \lambda \geq 0. \quad (19)$$

Choosing the negative identity for the penalty  $\text{pen}$ , one ends up with a sign-constrained version of the graphical lasso. We here refrain from the penalty approach. Instead, we argue for a post-processing procedure combining thresholding and re-fitting.

### 3.1. Hard thresholding and re-fitting

Suppose that the population precision matrix  $\Omega_* \in \mathcal{M}^p$  has few non-zero entries, i.e. the set  $\mathcal{E}^* = \{(j, k) : \omega_{jk}^* < 0\}$  as already defined in (17) has small cardinality. We may interpret  $\mathcal{E}^*$  as the edge set of the graph of positive partial correlations associated with  $\Omega_*$ . Our aims are recovery of  $\mathcal{E}^*$  and accurate estimation of  $\Omega_*$  under sparsity given a finite sample of i.i.d. observations. We suggest the following scheme.

1. We first compute the minimizer  $\widehat{\Omega}$  of (6) as initial estimate.
2. We apply hard thresholding to the off-diagonal entries, i.e. for some threshold  $t \geq 0$ , we let

$$\widehat{\Omega}(t) = (\widehat{\omega}_{jk}(t)) = \begin{cases} \widehat{\omega}_{jk} & \text{if } j = k, \\ I(-\widehat{\omega}_{jk} > t) \widehat{\omega}_{jk} & \text{if } j \neq k. \end{cases} \quad (20)$$

3. We estimate  $\mathcal{E}^*$  by  $\widehat{\mathcal{E}}(t) = \{(j, k) : \widehat{\omega}_{jk}(t) < 0\}$ .

Since  $\widehat{\Omega}(t)$  is in general no longer positive definite, we perform a re-fit subject to additional zero constraints on the off-diagonal entries as represented by  $\widehat{\mathcal{E}}(t)$ , that is we compute

$$\widehat{\widehat{\Omega}}(t) = \underset{\Omega \in \overline{\mathcal{M}^p}, \omega_{jk}=0 \forall (j,k) \notin \widehat{\mathcal{E}}(t), j \neq k}{\text{argmin}} -\log \det(\Omega) + \text{tr}(\Omega S). \quad (21)$$

In addition to being positive definite, the final estimator  $\widehat{\widehat{\Omega}}(t)$  potentially improves over  $\widehat{\Omega}$  regarding estimation of  $\Omega_*$  if  $\widehat{\mathcal{E}}(t) \supseteq \mathcal{E}^*$  and  $\widehat{\mathcal{E}}(t)$  is of small cardinality; see [56] for an analysis of precision matrix estimation subject to zero constraints on off-diagonal elements.

### 3.2. Justification

In the sequel, we provide some theoretical underpinning for the suggested approach. Successful identification of  $\mathcal{E}^*$  via thresholding entails that the initial estimate  $\widehat{\Omega}$  obeys the condition

$$\max_{(j,k), j \neq k} |\widehat{\omega}_{jk} - \omega_{jk}^*| \leq t, \quad \min_{(j,k) \in \mathcal{E}^*} |\omega_{jk}^*| > 2t. \quad (22)$$

We wish to take the threshold  $t$  as small as possible so that it is possible to detect even non-zero off-diagonal elements in  $\Omega_*$  of small absolute magnitude, but still large enough to filter out all pairs not in  $\mathcal{E}^*$ . Performance hence depends on the  $\ell_\infty$ -distance of off-diagonal entries of  $\widehat{\Omega}$  to those of  $\Omega_*$ . In the classic setting with  $p$  fixed as  $n \rightarrow \infty$ , consistency of  $\widehat{\Omega}$  can be established by using standard arguments.

**Proposition 1.** *Let  $x_1, \dots, x_n$  be i.i.d. realizations from a  $p$ -dimensional random vector  $X$  with precision matrix  $\Omega_*$ . Furthermore, suppose that  $X$  has finite fourth moments. Then, with  $\Omega_\bullet$  as defined in (13), the minimizer of the sign-constrained log-determinant divergence (6) satisfies  $\widehat{\Omega} = \Omega_\bullet + o_{\mathbf{P}}(1)$  as  $n \rightarrow \infty$  and  $p$  stays fixed.*

Note that if  $\Omega_* \in \mathcal{M}^p$ , we have  $\widehat{\Omega} = \Omega_* + o_{\mathbf{P}}(1)$ . In that case, for  $n$  large enough, there exists a threshold  $t$  such that (22) holds. In the modern setting with  $p$  being of the order of  $n$  or even  $p > n$ , the situation is less clear. Here, the use of the thresholding procedure is mainly justified by its strong empirical performance (cf. Section 5). In addition, we provide the very first step towards an understanding of what one observes empirically. Namely, we can show the following.

**Proposition 2.** *For  $\rho \in (0, 1)$ , let*

$$\Sigma_* = \text{bdiag} \left( \begin{pmatrix} 1 & \rho \\ \rho & 1 \end{pmatrix}, I_{p-2} \right), \quad \Omega_* = \text{bdiag} \left( \begin{pmatrix} \omega_{11}^* & \omega_{12}^* \\ \omega_{12}^* & \omega_{22}^* \end{pmatrix}, I_{p-2} \right),$$

*with  $\omega_{12}^* = -\rho/(1-\rho^2)$  so that  $\mathcal{E}^* = \{(1, 2), (2, 1)\}$  and  $\omega_{11}^* = \omega_{22}^* = 1/(1-\rho^2)$ . Denote*

$$B := \max_{1 \leq j, k \leq p} |s_{jk} - \sigma_{jk}^*|, \quad (23)$$

*where  $S = (s_{jk})$  is the sample covariance matrix (5) based on an i.i.d. sample whose population covariance equals  $\Sigma_*$ . Suppose that sign-constrained log-determinant divergence minimization (6) has a unique minimizer  $\widehat{\Omega}$  and that*

$B = o_{\mathbf{P}}(1)$  as  $n \rightarrow \infty$ . Then there exists constants  $c_1, c_2, c_3 > 0$  such that

$$\max_{(j,k) \notin \mathcal{E}^*, j \neq k} (-\widehat{\omega}_{jk}) \leq c_1 B. \text{ Moreover, if } \rho > c_2 B, \quad (-\widehat{\omega}_{12}) \geq (-\omega_{12}^*) - c_3 B > 0.$$

as  $n \rightarrow \infty$ . Consequently, if  $(-\omega_{12}^*) - (c_3 + c_1)B > 0$ , when applying thresholding with  $t = c_1 B$ , it holds that  $\widehat{\mathcal{E}}(t) = \mathcal{E}^*$ .

Proposition 2 studies the special case in which the graph associated with  $\Omega_*$  consists of a single edge. The ingredients of Proposition 2 are existence of  $\widehat{\Omega}$  (which may be concluded from Theorem 1), and a uniform bound  $B$  on the differences of the entries of  $S$  and those of  $\Sigma_*$ . Finite sample, high probability upper bounds on  $B$  in dependence on the decay of the tails of the underlying distribution can be found in [42]. In particular, for sub-Gaussian tails, one has  $B = O(\sqrt{\log(p)/n})$  with high probability, so that Proposition 2 asserts identification of  $\mathcal{E}^*$  even in the high-dimensional case, provided  $|\omega_{12}^*|$  is not too small in the sense that it stands out of the effective noise level.

A result for general  $\mathcal{E}^*$  is out of the scope of the present paper, though we conjecture that the rates of convergence for the elementwise  $\ell_\infty$ -error (22) are at least comparable to those available for  $\ell_1$ -regularization-based methods, e.g. [42, 9]. The proof techniques employed therein exploit the presence of explicit regularization, whereas regularization induced by the constraint  $\Omega \in \mathcal{M}^p$  is implicit and requires substantial extra work in order to be leveraged; see the proof of Proposition 2 in Appendix F.

*Thresholding vs. penalization.* We now briefly explain why we prefer thresholding over the commonly used penalization approach (19). First, sparsity-promoting penalty terms induce a bias, which adversely affects the identification of small, yet non-zero off-diagonal entries of  $\Omega_*$ . Second, thresholding is a direct way to achieve a desired level of sparsity: when one aims at a sparsity level of  $q$  percent, one simply keeps the  $q$  percent off-diagonal entries of  $\widehat{\Omega}$  that are largest in absolute magnitude, and sets the rest equal to zero. The sparsity level is not as easy to control when using penalization, because it cannot be read off directly what the resulting sparsity level for a specific choice of the regularization parameter will be. It is hence common to compute multiple solutions along a grid of specific values [3, 22]. However, this is unfavorable from a computational point of view, because one has to solve multiple instances of a challenging convex optimization problem.

## 4. Computational approach

Within this section, we present our computational approach for solving the sign- constrained log-determinant divergence minimization problem (6) numerically. As a convex optimization problem, it can be handled by general purpose solvers like `CVX` [23]. However, `CVX` becomes rather slow once the dimension  $p$  crosses 30. Note that the number of variables and constraints is quadratic in  $p$ , i.e. with  $p$  in the hundreds, the number of variables is in the ten thousands, and with  $p$  in the thousands, the number of variables is in the millions. It is clear that standard 'off-the-shelf' interior point methods as used in `CVX` are not suitable both with regard to runtime and memory requirements. We hence devise a customized solver for the problem.

### 4.1. Block coordinate descent

The algorithm that we propose follows the one pioneered in [3] to solve the graphical lasso problem, and gives rise to an analogous interpretation: just like the approach in [3] amounts to recursively solving  $\ell_1$ -penalized regression (lasso) problems, our algorithm amounts to recursively solving non-negative least squares regression (NNLS) problems. In view of this connection, optimization can be delegated to an arbitrary NNLS solver. Apart from conceptual simplicity and ease of implementation, the algorithm has a solid theoretical foundation as block coordinate descent scheme, so that existing theory can be leveraged to establish convergence. The approach solves problem up to  $p = 1000$  still reasonably fast, but comes with a rather sharp increase in runtime as  $p$  increases, with a complexity of  $O(p^4)$ .

### 4.2. Reduction to a linear complementarity/non-negative least squares problem

Algorithm 1 is a block coordinate descent scheme in which one variable block consisting of a single column/row is optimized at a time, while the remaining entries are kept fixed. This is cyclically repeated for all  $p$  blocks until a suitable stopping criterion is satisfied. The approach is appealing because it turns out that the sub-problems (24) are particularly easy to solve by means of a conversion to linear complementarity problems (25), for which efficient solvers exist. In the sequel, we show that the routine `SOLVE-BLOCK` indeed provides the solution of (24). We start by decomposing the determinant part as

$$\det \tilde{\Omega}^t(\omega_{jj}, \omega_j) = \det(\Omega_{jj}^t) \cdot \left( \omega_{jj} - \omega_j^\top \{\Omega_{jj}^t\}^{-1} \omega_j \right),$$



assuming for a moment that  $\Omega_{jj}^t \in \mathbb{S}_+^{p-1}$  as will be shown below. After taking logarithms, the first factor becomes a constant not depending on the optimization variables  $(\omega_{jj}, \omega_j)$  and can hence be omitted. Similarly, the trace term in (24) can be decomposed as

$$\text{tr}(\tilde{\Omega}^t(\omega_{jj}, \omega_j)S) = 2\omega_j^\top s_j + s_{jj}\omega_{jj} + \text{tr}(S_{jj}\Omega_{jj}^t),$$

where  $s_{jj}, s_j, S_{jj}$  are the components of a partitioning of  $S$  analogous to that of  $\Omega^t$ . The term  $\text{tr}(S_{jj}\Omega_{jj}^t)$  does not depend on the optimization variables

---

**Algorithm 1** Algorithm for problem (6)

---

**Input:** sample covariance matrix  $S$

**Initialization:**  $t \leftarrow 0$ ,  $\Sigma^t \leftarrow D(S)$ ,  $\Omega^t \leftarrow \{\Sigma^t\}^{-1}$ .

**while** stopping criterion not fulfilled **do**

**for**  $j = 1, \dots, p$  **do**

- Call routine SOLVEBLOCK below to obtain

$$(\tilde{\omega}_{jj}, \tilde{\omega}_j) \leftarrow \underset{\omega_{jj}, \omega_j}{\text{argmin}} - \log \det \tilde{\Omega}^t(\omega_{jj}, \omega_j) + \text{tr}(\tilde{\Omega}^t(\omega_{jj}, \omega_j)S) \quad (24)$$

$$\text{sb. to } \tilde{\omega}_j \leq 0, \tilde{\Omega}^t(\omega_{jj}, \omega_j) \in \overline{\mathbb{S}_+^p},$$

where, with the partitioning scheme (3),  $\tilde{\Omega}^t(\omega_{jj}, \omega_j) = \begin{pmatrix} \omega_{jj} & \omega_j^\top \\ \omega_j & \{\Omega_{jj}^t\} \end{pmatrix}$ .

- $\Omega^{t+1} \leftarrow \tilde{\Omega}^t(\tilde{\omega}_{jj}, \tilde{\omega}_j)$  and  $\Sigma^{t+1} \leftarrow \begin{pmatrix} s_{jj} & (\sigma_j^{t+1})^\top \\ \sigma_j^{t+1} & \Sigma_{jj}^t \end{pmatrix}$ ,

$$\text{with } \sigma_j^{t+1} = s_{jj}(\Omega_{jj}^t)^{-1}(-\tilde{\omega}_j).$$

**end for**

**return**  $(\hat{\Omega}, \hat{\Sigma})$ .

**end while**

---

**SOLVEBLOCK**

**Input:**  $\Sigma^t, S, j$ .

Solve the following linear complementarity problem in  $(\eta, \lambda)$  (recall (3)):

$$\left( \Sigma_{jj} - \frac{\sigma_j \sigma_j^\top}{s_{jj}} \right) \eta = \frac{s_j}{s_{jj}} + \lambda, \quad \eta \geq 0, \quad \lambda \geq 0, \quad \eta^\top \lambda = 0. \quad (25)$$

**return**  $\tilde{\omega}_j \leftarrow -\eta$ ,  $\tilde{\omega}_{jj} \leftarrow (1 + s_{jj}\tilde{\omega}_j^\top \Omega_{jj}^{-1} \tilde{\omega}_j)/(1 + s_{jj})$ .

---

and can be dropped as well. Altogether, we find that (24) is equivalent to the following optimization problem:

$$\begin{aligned} \min_{\omega_{jj}, \omega_j} & -\log(\omega_{jj} - \omega_j^\top \{\Omega_{jj}^t\}^{-1} \omega_j) + 2\omega_j^\top s_j + s_{jj}\omega_{jj}, \\ \text{sb. to } & \omega_j \leq 0, \quad \omega_{jj} - \omega_j^\top \{\Omega_{jj}^t\}^{-1} \omega_j \geq 0, \quad \omega_{jj} \geq 0, \end{aligned} \quad (26)$$

Observe that the constraint  $\tilde{\Omega}^t(\omega_{jj}, \omega_j) \in \overline{\mathbb{S}}_+^p$  is equivalent to the second and third constraint in (26) given  $\Omega_{jj}^t \in \mathbb{S}_+^{p-1}$ , recalling that a symmetric matrix is positive semi-definite if and only if all its principal minors are non-negative. Setting  $\log(x) = -\infty$  if  $x \leq 0$ , the second and third constraint can be dropped as long as  $\Omega_{jj}^t \in \mathbb{S}_+^{p-1}$ . The objective function in (26) consists of a linear part and the composition of the negative logarithm (which is convex and non-increasing) and a concave function (assuming again  $\Omega_{jj}^t \in \mathbb{S}_+^{p-1}$ ). Such a function is again convex ([7], p.84). We conclude that  $(\tilde{\omega}_{jj}, \tilde{\omega}_j)$  is a minimizer of (24) if and only if it satisfies the KKT optimality conditions of (26) given by

$$\begin{aligned} \frac{1}{\tilde{\omega}_{jj} - \tilde{\omega}_j^\top \{\Omega_{jj}^t\}^{-1} \tilde{\omega}_j} &= s_{jj}, \quad \frac{\{\Omega_{jj}^t\}^{-1} \omega_j}{\tilde{\omega}_{jj} - \tilde{\omega}_j^\top \{\Omega_{jj}^t\}^{-1} \tilde{\omega}_j} = -(s_j + \kappa), \\ \tilde{\omega}_j &\leq 0, \quad \kappa \geq 0, \quad \tilde{\omega}_j^\top \kappa = 0. \end{aligned} \quad (27)$$

where  $\kappa \geq 0$  is a Lagrangian multiplier. Substituting the first equation in (27) into the second one, we obtain

$$\{\Omega_{jj}^t\}^{-1} \tilde{\omega}_j = \frac{-(s_j + \kappa)}{s_{jj}}.$$

It is hence possible to solve the KKT system (27) for  $\tilde{\omega}_j$  first and then resolve for  $\tilde{\omega}_{jj}$ . This automatically ensures that  $\tilde{\omega}_{jj} - \tilde{\omega}_j^\top \{\Omega_{jj}^t\}^{-1} \tilde{\omega}_j > 0$  and in turn that  $\Omega^{t+1} \in \mathbb{S}_+^p$ . Applying this argument recursively, it follows that all iterates must be strictly positive definite, provided the initial iterate  $\Omega^0 = \{D(S)\}^{-1}$  is. Re-parameterizing  $\eta = -\tilde{\omega}_j$  and  $\lambda = \kappa/s_{jj}$ , solution of (26) respectively (27) boils down to solving

$$\{\Omega_{jj}^t\}^{-1} \eta = \frac{s_j}{s_{jj}}, \quad \eta^\top \lambda = 0, \quad \eta \geq 0, \quad \lambda \geq 0, \quad (28)$$

We finally recover (25) in Algorithm 1 from (28) by re-writing  $\{\Omega_{jj}^t\}^{-1}$  using Schur complements. Problem (28) is a so-called *monotone linear complementarity problem* ([4], Ch.11). It is not hard to handle (28), because it is

equivalent to the quadratic programming problem

$$\min_{\eta \geq 0} \frac{1}{2} \eta^\top \{\Omega_{jj}^t\}^{-1} \eta - \eta^\top s_j / s_{jj},$$

which is in turn equivalent to the non-negative least squares (NNLS) problem

$$\min_{\eta \geq 0} \frac{1}{2} \|b - A\eta\|_2^2, \quad A = \{\Omega_{jj}^t\}^{-1/2}, \quad b = \{\Omega_{jj}^t\}^{1/2} \frac{s_j}{s_{jj}}.$$

Consequently, (28) can be solved by one of the many existing solvers for the previous two problems. We use the block principal pivoting algorithm of [41], which operates directly on the linear complementarity problem and is experimentally the fastest method for strictly convex NNLS problems where the number of variables does not exceed a few thousands [48].

### 4.3. Properties

*Convergence.* We now state that Algorithm 1 converges to the unique minimizer  $\widehat{\Omega}$  of (6), existence provided (cf. Theorem 1).

**Theorem 3.** *Under the conditions of Theorem 1, the sequence of iterates of Algorithm 1 satisfies  $\lim_{t \rightarrow \infty} \Omega^t = \widehat{\Omega}$ .*

The statement can be derived as a consequence of general result regarding block coordinate descent in [6]. Regarding the speed of convergence, our experiments suggest a linear rate (see Figure 6). This observation is supported by theoretical work in [34].

*Computational complexity.* One complete cycle of block updates requires  $O(p^4)$  operations, with each call to SOLVEBLOCK amounting to  $O(p^3)$  operations. The workhorse in SOLVEBLOCK is block principal pivoting, in which a linear system of dimension  $p$  has to be solved per iteration. SOLVEBLOCK typically terminates after few iterations.

*Stopping criterion.* We suggest to stop Algorithm 1 once one comes close to KKT optimality. In view of (8), this can be quantified by means of the criterion

$$\begin{aligned} \varepsilon &= \max\{\varepsilon_1, \varepsilon_2\}, \quad \text{where } \varepsilon_1 = \max_{(j,k) \in \mathcal{E}^t} |\sigma_{jk}^t - s_{jk}|, & (29) \\ \varepsilon_2 &= \max_{(j,k) \notin \mathcal{E}^t} \max\{s_{jk} - \sigma_{jk}^t, 0\}, \quad \mathcal{E}^t = \{(j,k) : \omega_{jk}^t < 0\}. \end{aligned}$$

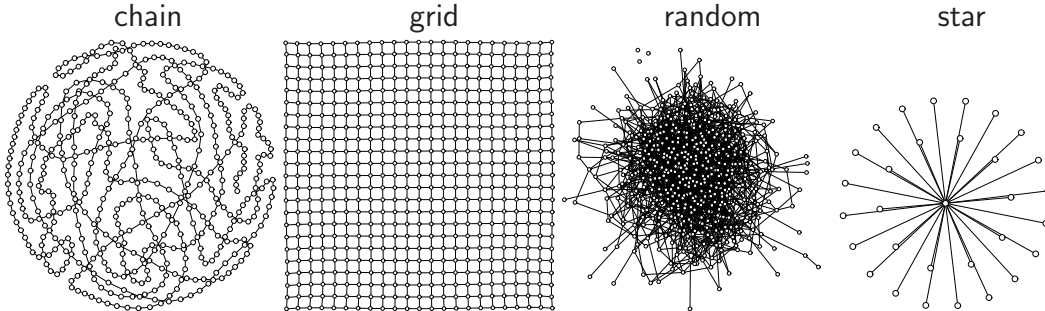


Figure 3: Graphs underlying a subset of the experimental setups.

## 5. Experiments

In the first part, we use synthetic datasets to study systematically the performance of our thresholding approach (Section 3) in the high-dimensional, sparse regime as compared to various competing methods proposed in the literature. In the second part, we present possible applications of precision matrix estimation under non-positivity constraints on the off-diagonal elements. Specifically, we consider learning of taxonomies and analysis of planar landmark data.

### 5.1. Synthetic data

*Data generation.* We generate two sets of i.i.d. samples  $x_1, \dots, x_n$  respectively  $\tilde{x}_1, \dots, \tilde{x}_n$  from a multivariate Gaussian distribution with mean zero and precision matrix  $\Omega_* \in \mathcal{M}^p$  according to one of the setups below. The first sample  $\{x_i\}_{i=1}^n$  is used to obtain the sample covariance matrix  $S = \frac{1}{n} \sum_{i=1}^n x_i x_i^\top$  (assuming the mean to be known), which is the input for all methods under comparison. The second sample  $\{\tilde{x}_i\}_{i=1}^n$  is kept aside and used only for hyperparameter selection. The parameter  $n$  is chosen in a setup-specific manner (see below).

*chain.* We use an AR(1)-model (cf. example (2) in Section 2.3) with positive parameter, setting  $\Sigma_* = (\sigma_{jk}^*) = (0.9^{|j-k|})$ ,  $j, k = 1, \dots, p = 500$ . The conditional independence graph encoded by  $\Omega_*$  is a chain.

*grid.* We set  $\tilde{\Omega}_* = \delta I - B$ , where  $B$  is the adjacency matrix of a 2d-grid (cf. Figure 3) of size  $p = 23 \cdot 23 = 529$ , and  $\delta = 1.05\lambda_1(B)$ . We then set  $\Omega_* = D\tilde{\Omega}_*D$ , where  $D$  is a diagonal matrix chosen such that  $\Sigma_* = \Omega_*^{-1}$  has unit diagonal entries.

*grid(3)*. As for 'grid', but with  $B$  replaced by the adjacency matrix of a 3d-grid of size  $p = 8 \cdot 8 \cdot 8 = 524$ .

*random*. As for 'grid', but with  $B$  replaced by a binary symmetric matrix of dimension  $p = 500$  having zero diagonal and one percent non-zero off-diagonal entries, generated uniformly at random.

*star*. We set  $\Sigma_* = \begin{pmatrix} 1 & \rho^\top \\ \rho & I + \rho\rho^\top \end{pmatrix} \in \mathbb{S}_+^{500}$ , where  $\rho = 0.6 \cdot \underbrace{(1, \dots, 1)}_{d \text{ times}}, 0, \dots, 0 / d^{1/4}$

( $d \in \{10, 15, 20, 25, 30\}$ ), so that  $\Omega_* = \begin{pmatrix} D & -\rho^\top \\ -\rho & I \end{pmatrix}$ , with  $D = 1 + \|\rho\|_2^2$ .

*decay*. Unlike the previous setups,  $\Omega_*$  is no longer sparse. Instead, its entries exhibit an exponential decay away from the off-diagonal according to  $\omega_{jk}^* = (-1)^{I(j \neq k)} \exp(-|j - k| \cdot 6/5)$ ,  $j, k = 1, \dots, p = 500$ .

Each setup is run for five different values of  $n$  (with the exception of 'star', where  $d$  varies while  $n$  is fixed to 500, see Figure 4). For each setup and each value of  $n$ , 50 replications are considered and performance is measured in the form of averages over these replications. To assess performance with regard to the recovery of the graph structure associated with  $\Omega_*$  (or, equivalently, recovery of the set  $\mathcal{E}^* = \{(j, k) : \omega_{jk}^* < 0\}$ ), we compute Matthew's correlation coefficient (MCC) defined by

$$\text{MCC} = (\text{TP} \cdot \text{TN} - \text{FP} \cdot \text{FN}) / \{(\text{TP} + \text{FP})(\text{TP} + \text{FN})(\text{TN} + \text{FP})(\text{TN} + \text{FN})\}^{1/2},$$

with TP, FN etc. denoting true positives, false negatives etc. The larger the criterion, the better the performance. Estimation of  $\Omega_*$  is evaluated by the error in spectral norm  $\|\Omega_* - \hat{\Omega}\|$ . We also report the Kullback-Leibler (KL) divergence  $D(\Omega_* \parallel \hat{\Omega}) = \log \det(\Omega_*) - \log \det(\hat{\Omega}) + \text{tr}(\hat{\Omega}\Sigma_*) - p$ .

*Methods compared*. In order to thoroughly benchmark our approach, our comparison includes various state-of-the-art methods in sparse precision matrix estimation and structure learning of GMRFs.

*attr*. We use the abbreviation 'attr' (mnemonic for attractive random field) to refer to the sign-constrained log-determinant divergence minimization plus thresholding approach as described in Section 3. The threshold  $t$  is chosen with the help of the separate validation set  $\{\tilde{x}_i\}_{i=1}^n$  in the following manner. Given the initial estimate  $\hat{\Omega}$ , we compute the  $q$ -quantiles of its off-diagonal entries,  $q \in \{0.7, 0.8, 0.9, 0.95, 0.99, 1, q^*\}$ , where  $q^* = 1 - |\mathcal{E}^*| / (p \cdot (p - 1) / 2)$

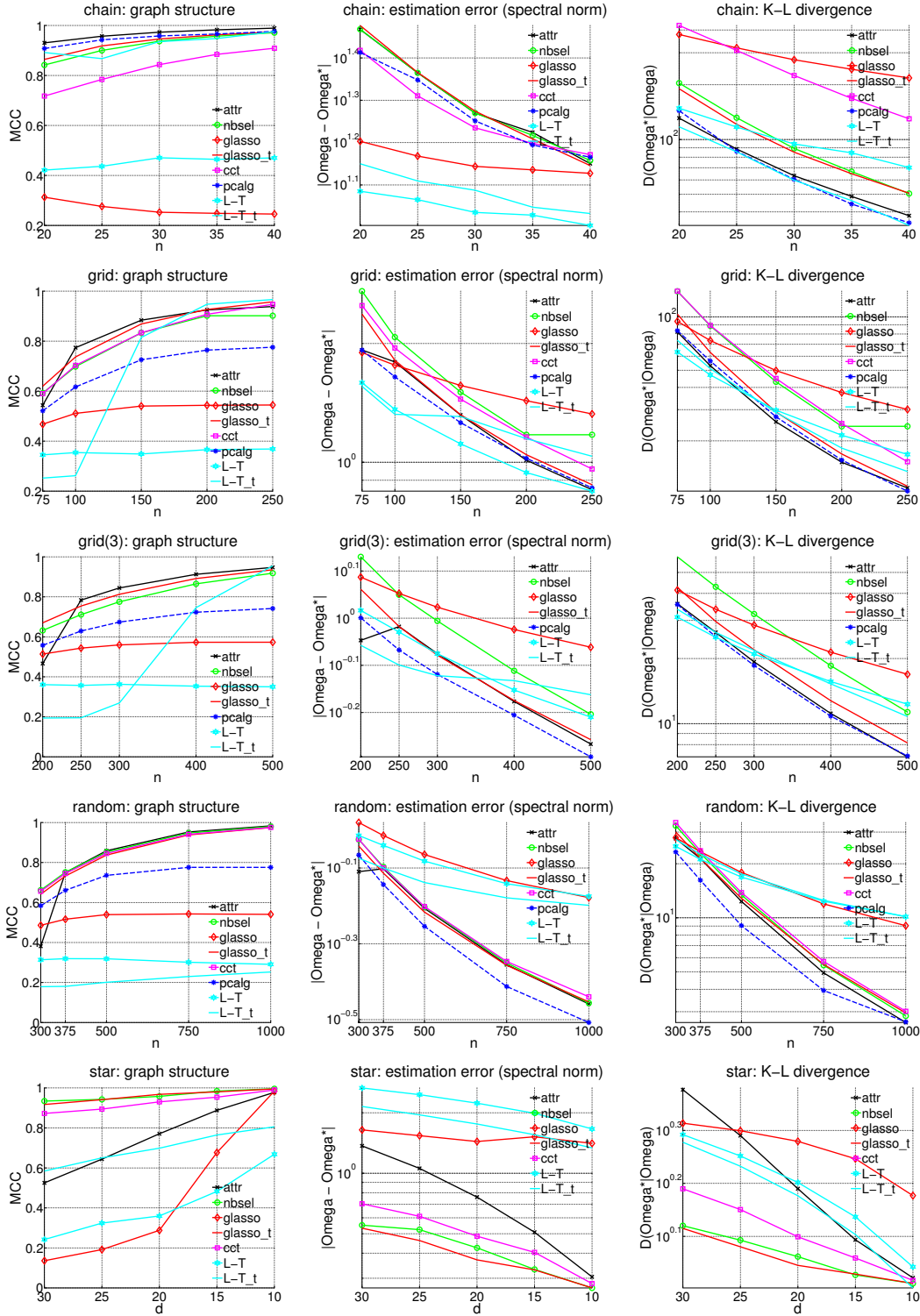


Figure 4: Average performance over 50 replications. Left to right: performance measures; top to bottom: settings under consideration. For spectral norm error and K-L divergence, a log-scale is used for both axes.

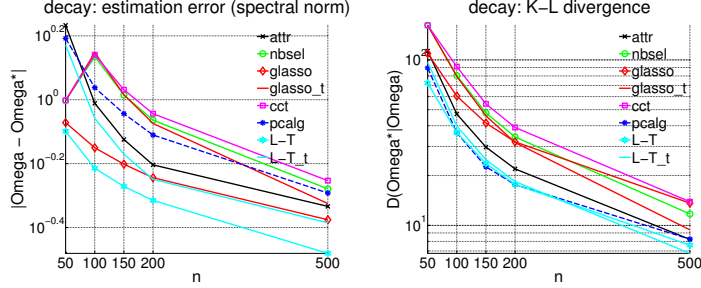


Figure 5: Note that for the setting 'decay'  $\Omega_*$  is not sparse; hence, we do not report MCC.

is the quantile corresponding to the smallest non-zero off-diagonal entry in  $\Omega_*$ . We then compute the loss on the validation set

$$-\log \det(\widehat{\Omega}(t)) + \text{tr}(\widehat{\Omega}(t)\tilde{S}), \quad \tilde{S} = \frac{1}{n} \sum_{i=1}^n x_i x_i^\top. \quad (30)$$

based on the re-fitted estimator (21), with  $t$  taken from the above quantiles, and pick the value of  $t$  for which (30) is minimized.

*glasso*. The graphical lasso is defined as minimizer of the  $\ell_1$ -penalized log-determinant divergence

$$\min_{\Omega \in \mathbb{S}_+^p} -\log \det(\Omega) + \text{tr}(\Omega S) + \lambda \sum_{(j,k): j \neq k} |\omega_{jk}|, \quad \lambda \geq 0.$$

Following [56], the parameter  $\lambda$  is chosen from the set  $\{0.01, 0.05, 0.1, 0.3, 0.5, 1, 2, 4, 8, 16\} \cdot \sqrt{(\log(p)/n)}$  such that the loss on the validation set as in (30) is minimized. We also consider a thresholding plus refitting variant of the *glasso*, denoted by *glasso-t*. Thresholding and refitting proceeds as for 'attr' with  $\widehat{\Omega}(\lambda^*)$  as initial estimator, where  $\widehat{\Omega}(\lambda^*)$  denotes the *glasso* estimator with  $\lambda = \lambda^*$  chosen as described above.

*L-T*. Lake and Tenenbaum [32] consider the class of precision matrices  $\mathcal{L}_I^p$  (2) that can be written as a Laplacian matrix plus a multiple of the identity. Sparsity is promoted via an  $\ell_1$ -penalty as for the 'glasso', which yields the following optimization problem.

$$\min_{\Omega \in \mathcal{L}_I^p} -\log \det(\Omega) + \text{tr}(\Omega S) + \lambda \sum_{(j,k): j \neq k} (-\omega_{jk}), \quad \lambda \geq 0.$$

Recall that  $\mathcal{L}_I^p \subset \mathcal{M}^p$  so that  $\Omega \in \mathcal{L}_I^p \Rightarrow \omega_{jk} \leq 0, j \neq k$ . The parameter  $\lambda$  is chosen in the same manner as for the 'glasso'. Likewise, we consider a version with thresholding and refitting, denoted by *L-T-t*.

The following three approaches only try to infer the graph structure of the conditional independence graph, i.e. their output is an estimate  $\widehat{\mathcal{E}}$  of  $\mathcal{E}^* = \{(j, k) : \omega_{jk}^* < 0\}$ . The precision matrix is estimated as

$$\widehat{\Omega} = \underset{\Omega \in \overline{\mathbb{S}}_+^p, \omega_{jk}=0 \forall (j,k) \notin \widehat{\mathcal{E}}, j \neq k}{\operatorname{argmin}} -\log \det(\Omega) + \operatorname{tr}(\Omega S),$$

provided the minimizer exists, see e.g. [51] for sufficient conditions.

*nbsel*. Neighborhood selection as proposed in [38] tries to infer the graph structure by node-wise  $\ell_1$ -penalized linear regression in which one variable is regressed on the remaining ones. Pairs of variables are connected by an edge whenever at least one of the two associated regression coefficients is nonzero. We use a refined version of neighborhood selection [56], in which hard thresholding is applied to the node-wise regression coefficients. Following [56], the regularization parameter for the node-wise  $\ell_1$ -penalized regressions is chosen from the grid  $\{0.01, 0.05, 0.1, 0.3, 0.5, 1, 2, 4, 8, 16\} \cdot \sqrt{(\log(p)/n)}$  to minimize the mean squared prediction error on the validation set over all  $p$  regression problems. Subsequent thresholding is performed according to the scheme used for 'attr'.

*cct*. In the conditional covariance testing approach of [2] one computes for all pairs  $(j, k)$ ,  $j \neq k$ , empirical conditional covariances  $\widehat{\sigma}_{jk|C} = s_{jk} - S_{jC}^\top S_{CC}^{-1} S_{Ck}$ , where the conditioning set  $C$  ranges over all subsets  $\mathcal{C}(\eta)$  of cardinality at most  $\eta \geq 0$ , which is the tuning parameter of the approach. One then obtains  $\theta_{jk} = \min_{C \subseteq \mathcal{C}(\eta)} \widehat{\sigma}_{jk|C}$  and connects  $j$  and  $k$  by an edge if  $\theta_{jk}$  exceeds a suitable threshold (regarding the choice of threshold, we proceed as for 'attr'). The computational complexity of the procedure is  $O(p^{\eta+2})$  and recovery of  $\mathcal{E}^*$  according to the analysis in [2] requires  $\eta$  to be chosen as least as large as the size of the minimum vertex separator in the conditional independence graph over all pair of edges. For the chain and star graph,  $\eta = 1$ , for the grid  $\eta = 2$  and for grid(3),  $\eta = 3$  (which is not considered anymore for computational reasons), and 'cct' is run with the correct choice of  $\eta$  with knowledge about the underlying graph. For 'random' and 'decay',  $\eta$  is set to one.

*pcalg*. The PC algorithm [50] is an iterative procedure for inferring pairs of variables of zero partial correlation. The approach has been further developed and analyzed in the context of high-dimensional data in [27]. In each



$n/d$	chain		grid		grid(3)		random		star		decay	
	20	40	75	250	200	500	300	1000	30	10	50	200
attr	9.4	6.4	2.7	2.6	1.3	1.3	1.5	1.2	0.6	0.6	0.8	1
nbsel	6	6.2	5.8	4.7	4.4	4.1	4.1	2.6	4	4.1	7.6	7.1
glasso	8.2	10.1	12	11.9	11.4	4.4	10.9	3.9	3	3	12	14.6
L-T	6.7	8.5	7.4	5.2	6.8	5.5	6.4	5.1	8.8	9.7	7.9	5.5
cct	16.3	16.5	37.5	38.7	—	—	31.1	32	21.8	21.8	34.9	35.4
pcalg	0.6	0.2	0.2	0.2	0.2	0.4	0.2	1.4	0.2	0.2	0.2	0.2

Table 1: Median running times (in 100s) for solving one problem instance for the lower and upper ends of the range for  $n$  (resp.  $d$ ).

iteration, a series of tests for zero conditional covariances of increasing order, starting from marginal covariances, is performed. Structural consistency requires *faithfulness* of the underlying distribution [50]. In Appendix G, we prove that if  $\Omega_* \in \mathcal{M}^p$ , faithfulness holds, which justifies the use of the PC algorithm for the problem at hand. The significance level of the conditional independence tests is chosen from the grid  $\{0.001, 0.005, 0.01, 0.02, 0.05, 0.1\}$  to minimize the loss on the validation set. For the star graph, the PC algorithm is not run for computational reasons (in fact, its complexity depends on the maximum vertex degree of the conditional independence graph).

*Discussion: statistical performance.* Inspecting Figures 4 and 5, we find that the proposed approach performs competitively throughout; for two settings ('chain' and 'random'), it is among the top competitors. This is rather remarkable, given the fact that our approach is applied in high-dimensional settings without any explicit form of regularization employed in the first stage of estimation. A drop in performance is observed for 'star' as the vertex degree  $d$  becomes larger, for 'decay', and grid/grid(3) at the bottom end of the range considered for the sample size. The comparatively weak performance for 'star' indicates a sub-optimal dependence of the approach on the maximum vertex degree, which is, besides the overall sparsity of  $\Omega_*$ , a second parameter known to affect performance of sparse precision matrix estimation methods, see e.g. [42, 56, 9].

A general conclusion one can draw from the figures is that all two-stage estimation procedures perform better than the 'glasso' and 'L-T' (each without thresholding), excluding the non-sparse setting 'decay'.

*Discussion: running times.* The method of choice should not only have good statistical properties, but should as well be favourable in terms of computa-

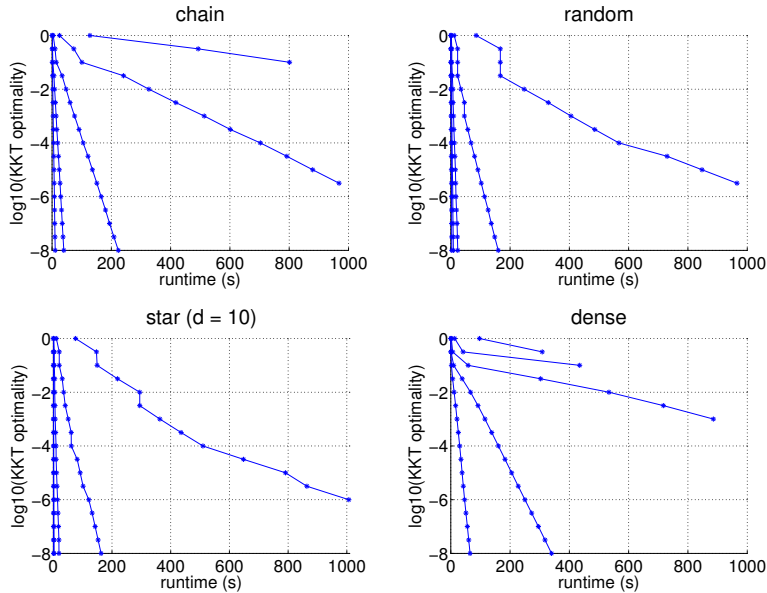


Figure 6: Empirical assessment of the speed of convergence of the block coordinate descent algorithm of Section 4. The five different trajectories per plot represent different  $p$ 's ranging from  $2^5$  to  $2^{10}$ , with faster convergence corresponding to smaller  $p$ .

tion. For this reason, we report the results of a small runtime comparison in Table 1. The running times reported there only refer to the first stage of estimation (including possible hyperparameter tuning), but excluding possible re-estimation steps given an estimate of the graph structure. Apart from 'pcalg', for which we use the R implementation [28], all methods are run under MATLAB. For 'glasso' and 'cct' publicly available code is used [31, 1]. We use code from [46] to solve the  $\ell_1$ -penalized regression problems arising for 'nbsel'. For 'attr', we have implemented the coordinate descent approach of Section 4. An own algorithmic approach based on projected gradient is used for L-T, which will be reported elsewhere. Table 1 reveals that while 'cct' is a theoretically sound approach which has also been seen to perform well empirically, it falls short in terms of runtime. The comparison is headed by 'pcalg', which outperforms all competitors by one order of magnitude; however, its computational complexity depends on the maximum degree of the graph, which becomes a severe issue for the setting 'star'. On average, 'attr' has smaller running times than the methods employing regularization ('nbsel', 'glasso' and 'L-T'), since no hyperparameter has to be set. The

speed of convergence of our computational approach has been investigated in a separate series of experiments whose results are displayed in Figure 6. For each of the four settings with  $p$  ranging from  $2^6$  to  $2^{10}$ , we measure the time required to achieve a certain level of KKT optimality as given in (29). The times reported in the figure are medians over ten replications obtained per setting. We use the following sample sizes:  $n = 40$  for 'chain',  $n = 1000$  for 'random', and  $n = 500$  for 'star' and 'dense'. For 'dense', the only of the four settings which is exclusively considered for the runtime analysis,  $\Omega_* = (0.3 \cdot I + 0.711\mathbf{1}\mathbf{1}^\top)^{-1}$ . Figure 6 suggest that our approach exhibits a linear rate of convergence, but does not scale well with  $p$  as already indicated in Section 4. Moreover, the speed of convergence visibly depends on the structure of  $\Omega_*$ , with 'dense' being the most difficult setting and 'star' as well as 'random' being easier than 'chain'.

### 5.2. Learning Taxonomies

In the next two paragraphs, we conduct an analysis performed in [32] where precision matrices of the form (2) are considered.

*Mammals dataset.* The dataset contains  $n = 85$  biological properties of  $p = 50$  mammals. The dataset is the outcome of a study [39], in which participants were asked to provide scores quantifying the relative strength of association between each mammal and the set of biological properties concerning anatomy, behaviour and living conditions on a scale ranging from 0 (no association) to 100 (perfect association). This yields a data matrix  $X = (x_{ij})$  with  $x_{ij}$  as the mean relative strength of association between property  $i$  and mammal  $j$ , and in turn a sample covariance  $S = \tilde{X}^\top \tilde{X}/n$ , where  $\tilde{X}$  results from  $X$  by centering its columns. The goal is to use the given data to infer a graphical representation of the 50 mammals serving as a taxonomy. We here compare approaches to sparse precision matrix estimation and the resulting graphs associated with the *negative* off-diagonal elements. Note that it is not meaningful to include edges corresponding to positive off-diagonal entries, since these edges would not be interpretable in the context of taxonomic reasoning. It still may make sense not to impose sign constraints in estimation, and to construct the graph only from the negative entries, because as discussed in Section 2.3, sign-constrained estimation may lead to a bias even for the underlying negative entries. We here compare the graphical lasso, Tikhonov regularization, a tree model, thresholding of  $S^{-1}$ , the method suggested in [32] ('L-T'), and our sign-constrained approach, among which only the latter two impose sign constraints. Tikhonov

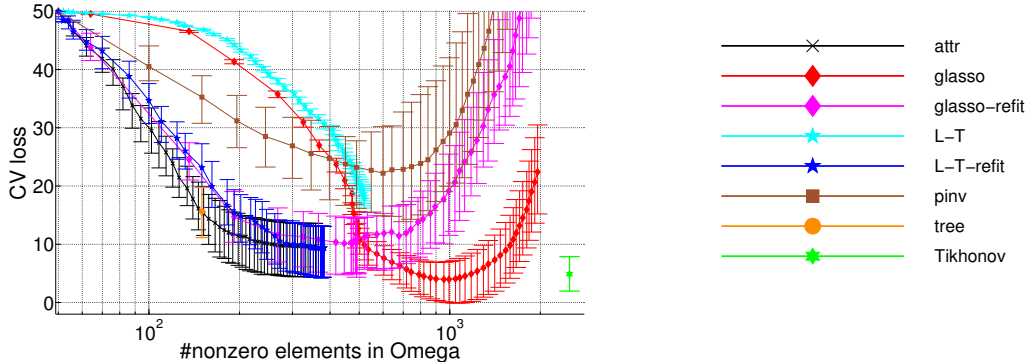


Figure 7: Cross-validated loss on the mammals dataset in dependency of the sparsity of the estimates. Upper and lower bars indicate the maximum respectively minimum loss over the ten random partitionings of the set of observations into ten folds, while points indicate medians. For the tree model ('tree') and Tikhonov regularization ('Tikhonov') the number of non-zeroes is constant, and three lines/points depict minimum, median (thick) and maximum. 'attr': attractive (sign-constrained) estimation; 'glasso(-refit)': graphical lasso (with re-fitting given the zero pattern); 'L-T(-refit)': method of Lake and Tenenbaum (with re-fitting given the zero pattern); 'pinv': thresholding of the (pseudo)-inverse.

regularization provides an estimate  $\hat{\Omega} = ((1 - \alpha)S + \alpha I)^{-1}$ , where  $\alpha \in [0, 1]$  is a tuning parameter. For the tree model, we restrict the graph associated with the precision matrix to be a tree, and the estimate is obtained with the help of the Chow-Liu algorithm [12]. In order to judge the usefulness of the sign-constraints, we include thresholding and re-fitting as described in Section 3, with the difference that  $S^{-1}$  is used as initial estimator. Performance is quantified by computing the cross-validated loss defined analogously to (30). Regarding cross-validation, we consider ten folds and ten random partitionings into folds. We consider 50 different values of the respective tuning parameters corresponding to varying levels of sparsity of the estimates (except for Tikhonov regularization, which yields fully dense estimates, and we report the minimum loss over all choices of  $\alpha$ ) as displayed in Figure 7. Our sign-constrained approach performs best for high levels of sparsity, which is the regime of interest here. Interestingly, in the range of 150 to 200 non-zero entries, both cross-validated loss and graph come rather close to the tree model (see Figure 9), which is conventionally used for depicting taxonomic relationships. In general, taxonomies are not required to have a tree structure. As pointed out in [32], the data set under consideration contains several features concerning e.g. habitat or appearance that may induce associations between species that would not be linked in an evolutionary tree. Unlike the

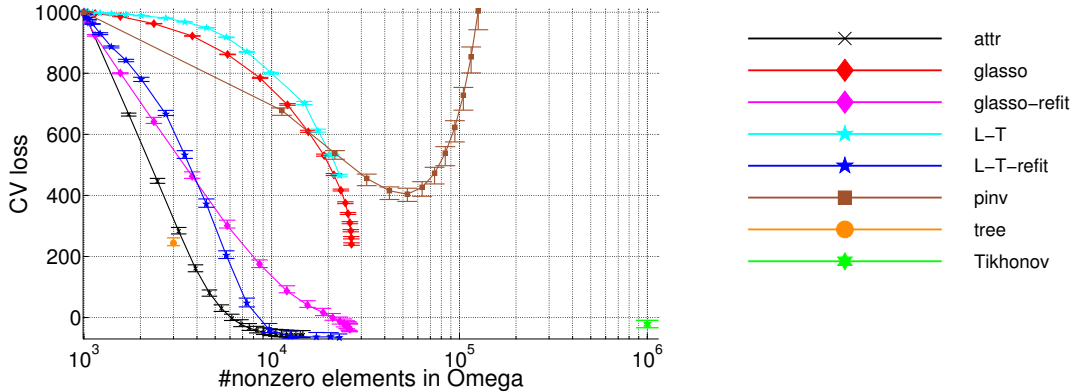


Figure 8: Cross-validated loss on the concepts dataset in dependency of the sparsity of the estimates. The annotation is as for Figure 7 above.

tree model, an attractive model is not constrained in the number of edges and may hence constitute a more flexible alternative; this has to be kept in mind when comparing the cross-validated loss of the two approaches. All edges of the Chow-Liu tree are associated with positive partial correlations, which supports the use of an attractive model. The latter yields several extra edges relative to the tree, some of which are less intuitive (elephant and pig, hamster and chihuahua, weasel and wolf). The sign constraints appear to be limiting in the sense that a visibly lower cross-validated loss can be achieved by methods not imposing sign constraints. However, this concerns a regime in which the estimates are no longer sparse and thus less interpretable.

*Concepts dataset.* The analysis in the present paragraph is of the same spirit as the previous one, with the important difference that the dataset under consideration is high-dimensional ( $n = 218$ ,  $p = 1000$ ). The goal is to infer a semantically meaningful graph-based representation of 1000 concepts falling into a diverse set of categories such as food, buildings, animals, clothes or other consumer goods, with the help of answers given to 218 questions concerning various attributes. The answers are on a five-point scale from 'clearly no' to 'clearly yes', obtained from Amazon Mechanical Turk [26]. For simplicity, we treat the data as if the scale level were metric. The analysis is conducted in the same way as the previous one, with two minor modifications. In order to reduce computing times, five-fold cross-validation is used and only 20 different values are considered for the tuning parameters.

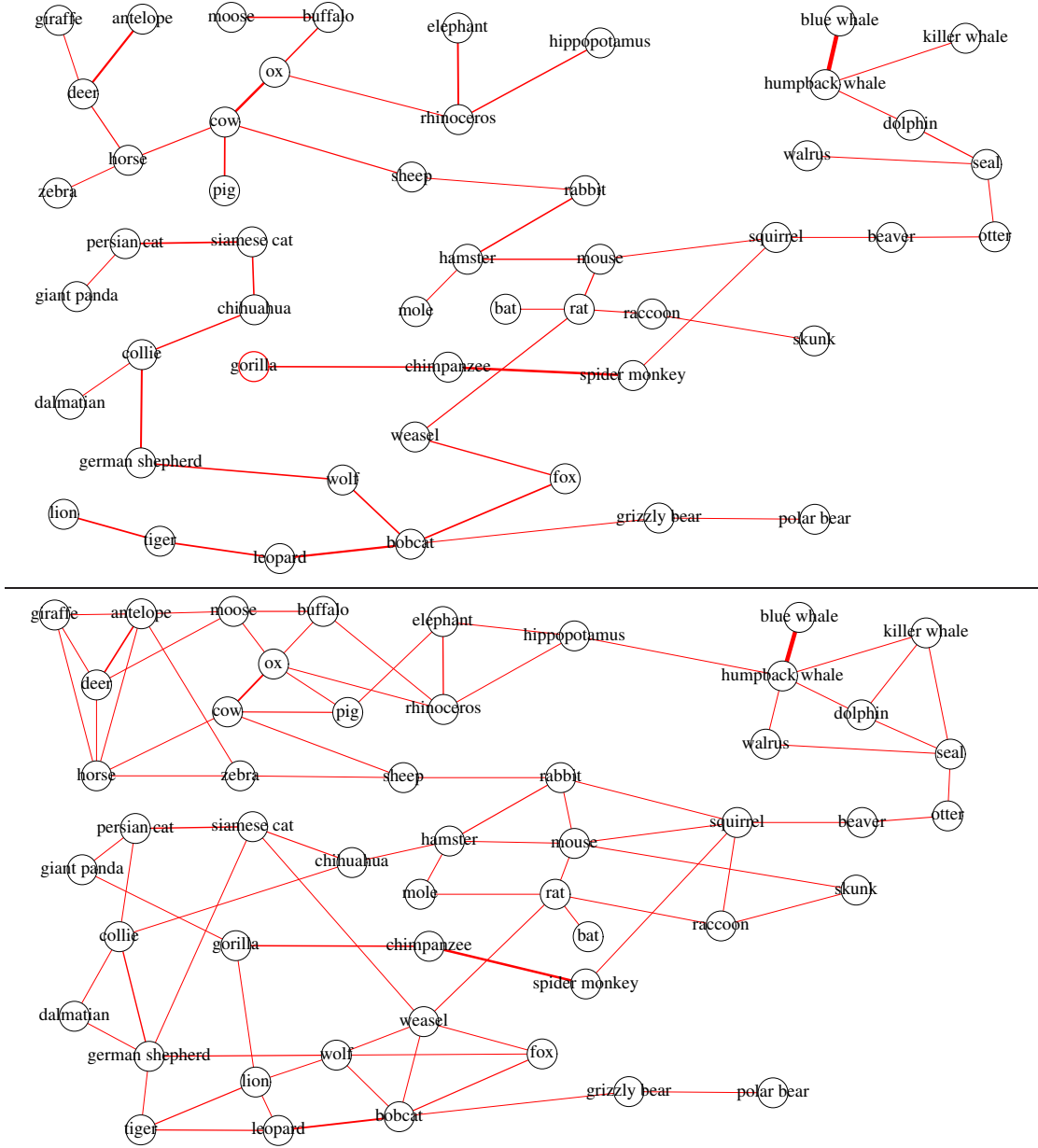


Figure 9: Graphs for the mammals dataset. Top: graph of the tree model having  $p-1 = 49$  edges (all of which are associated with positive partial correlations) and a median cross-validated loss of 15.63. Bottom: graph of the attractive model after thresholding having 83 edges and a median cross-validated loss of 10.88, with the threshold set to the 0.47-quantile of the absolute values of the non-zero off-diagonal entries in  $\hat{\Omega}$ . Edge widths are proportional to the absolute values of the corresponding entries in the precision matrices.



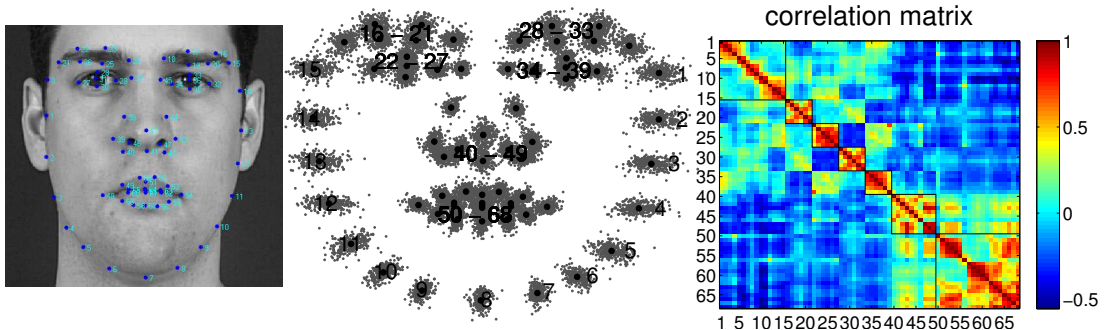


Figure 11: Landmarking scheme (left), scatterplot of landmark points and their numerical labels (middle; contour: landmarks 1-15, eyebrows: landmarks 16-21 and 28-33, eyes: landmarks 22-27 and 34-39, nose: landmarks 40-49, mouth: landmarks 50-68) and correlation matrix corresponding to the covariance matrix  $S^{\text{lm}}$  of the training set. The squares indicate the blocks corresponding to the landmark groups for contour, eyebrows, eyes, nose and mouth.

### 5.3. Covariance modeling of landmark data

In the present section, we consider the use of positive definite  $M$ -matrices for modeling the interdependence of planar landmarks contained in the face image dataset XM2VTS available from [13]. The concept of our analysis has been inspired by a similar one in [24], where, however, different datasets and methods are employed. The full dataset comprises frontal photos of 295 individuals collected over four sessions, with two shots per individual in each session. A set of  $p = 68$  landmarks is collected for each photo (cf. left panel of Figure 11). We here restrict ourselves to the first session, using the firsts of the two shots as the training set and the second ones as test set. Landmark data falls into the domain of statistical shape analysis [17], and we apply the usual steps developed in this area (centering, scaling, and generalized Procrustes analysis) to process the raw data. The thus pre-processed landmark data is given by  $(x_{ij}, y_{ij})$ ,  $i = 1, \dots, n$ ,  $j = 1, \dots, p$ , where  $(x_{ij}, y_{ij})$  is the coordinate pair of the  $j$ -th landmark of the  $i$ -th observation (cf. middle panel of Figure 11). As starting point, we consider a factored covariance model of the form  $\Sigma_* = \Sigma_*^{\text{xy}} \otimes \Sigma_*^{\text{lm}}$ , where  $\Sigma_*^{\text{xy}} \in \mathbb{S}_+^2$  represents the covariance between  $x$  and  $y$  coordinates and  $\Sigma_*^{\text{lm}} \in \mathbb{S}_+^{68}$  models the covariance between landmarks (cf. [17], p.167). While this model is restrictive, since it requires the structure of variability to be the same at each landmark, it is convenient for interpretation at the level of landmarks. Instead of fitting such a model



directly from the joint sample covariance  $S = \begin{pmatrix} S_{xx} & S_{xy} \\ S_{yx} & S_{yy} \end{pmatrix}$ , we consider a simpler approach that is sufficient for our purpose here. We first determine

$$(S^{xy}, S^{lm}) = \underset{\Sigma^{xy} \geq 0, \Sigma^{lm} \geq 0}{\operatorname{argmin}} \|S - \Sigma^{xy} \otimes \Sigma^{lm}\|_F \quad (31)$$

and work subsequently only with  $S^{lm}$  in the sequel as input for precision matrix estimation methods. Omitting further details here, solving (31) does not constitute an obstacle, as it turns out that this can be done essentially in closed form. The mode of evaluation is as in the previous subsection, but we report the loss on the test set instead of a cross-validated loss. In Figure 13, we compare the graphical lasso and our approach in terms of the graph structure they provide for several levels of sparsity. Interestingly, the graphs are rather similar as long as both of them contain only few edges connecting landmarks belonging to the distinct parts of the face (eyes, eyebrows, nose, mouth) and a chain along the boundary of the face. As the graphs become denser, edges appear between the different parts. For the graphical lasso, a considerable fraction of these edges correspond to negative partial correlations.

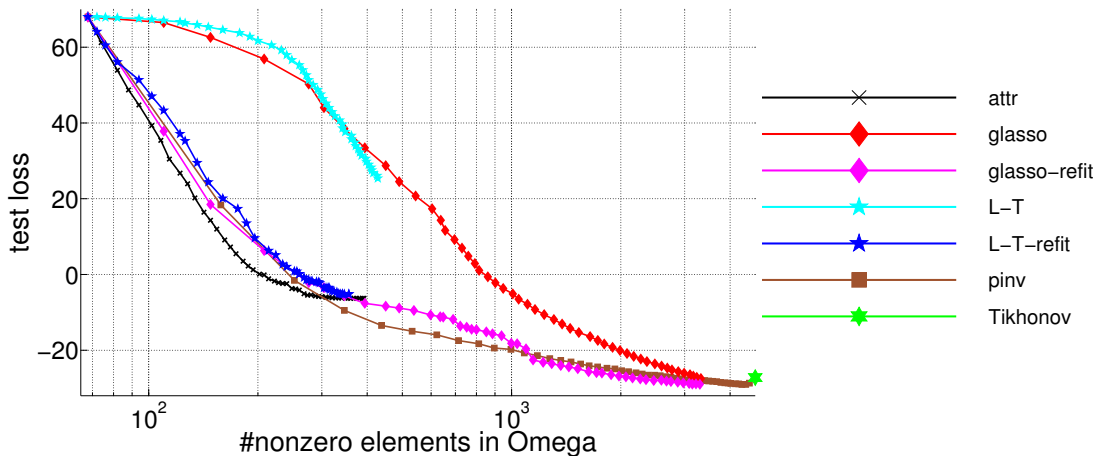


Figure 12: Test loss on the landmark dataset in dependency of the sparsity of the estimates. The annotation is as for Figure 7 above.

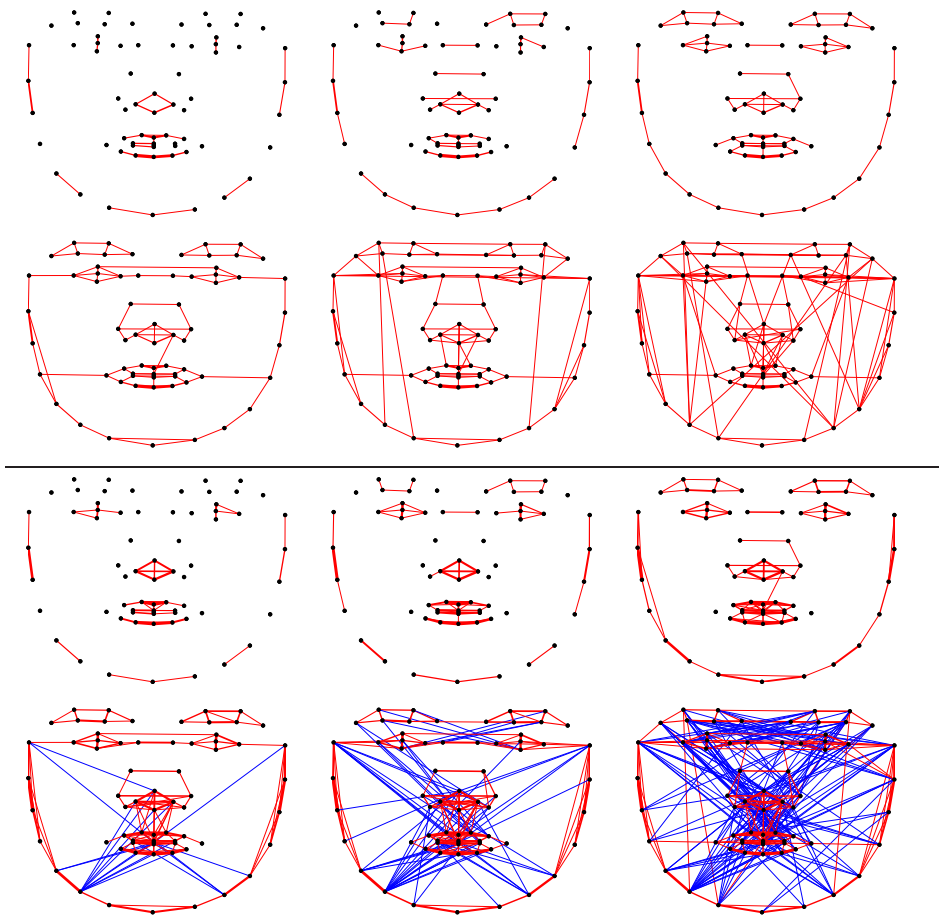


Figure 13: Graphs for the landmark dataset for six different levels of sparsity. Top: attractive model. Bottom: graphical lasso. Edge widths are proportional to the absolute values of the corresponding entries in the estimated precision matrix, and the edge colour represents their signs (red: negative sign, blue: positive sign).

## 6. Summary

The paper has addressed the use of non-positivity constraints on the off-diagonal part in precision matrix estimation. We have pointed out that the sign constraints constitute a severe restriction from the perspective of modelling, but also a blessing from the perspective of estimation. Specifically, we have provided evidence indicating that regularization is no longer compulsory in a high-dimensional regime, and that a simple post-processing (thresholding) gives rise to well-interpretable results on real world data sets.

The theoretical results of this paper fall behind the empirical findings. Proving structural consistency is left for future research, as is the development of a faster algorithm that scales more favourably with respect to the number of variables.

*Acknowledgments.*

We would like to thank Brendan Lake for providing us the datasets analyzed in Section 5.

## Appendix A. Proof of Theorem 1

The proof relies on a characterization of the spectrum of a positive definite  $M$ -matrix, which is based on the following results extracted from [5] and [4]. In the sequel, we write  $r(A) = \max\{\lambda_1(A), -\lambda_p(A)\}$  for the spectral radius of a symmetric matrix  $A \in \mathbb{R}^{p \times p}$  with spectrum  $\lambda_1(A) \geq \dots \geq \lambda_p(A)$ .

**Lemma A.1.**  $\Omega \in \overline{\mathcal{M}^p}$  (resp.  $\Omega \in \mathcal{M}^p$ ) if and only if there exists  $B \geq 0$ ,  $B = B^\top$  and  $\delta \in [r(B), \infty)$  (resp.  $\delta \in (r(B), \infty)$ ) such that  $\Omega = \delta I - B$ .

**Definition A.1.** A matrix  $A$  is said to be irreducible if there exists a permutation matrix  $\Pi$  such that

$$\Pi A \Pi^\top = \begin{pmatrix} A_1 & A_2 \\ 0 & A_3 \end{pmatrix}.$$

**Remark A.1.** Note that if  $A$  is symmetric,  $\Pi A \Pi^\top$  is symmetric as well. Consequently, if  $A$  is symmetric and reducible, it must be a block diagonal matrix.

**Theorem A.1.** (Perron–Frobenius) Let  $A \geq 0$  be a square irreducible matrix. Then  $r(A)$  is a positive, algebraically simple eigenvalue of  $A$ , and  $A$  has a corresponding positive eigenvector.

**Remark A.2.** If  $A \geq 0$  is symmetric and reducible, then, after a suitable permutation,  $A$  is block diagonal (cf. Remark A.1) with blocks  $A_1, \dots, A_K$ , say, and the Perron-Frobenius Theorem applies to each block. The positive eigenvectors corresponding to  $r(A_1), \dots, r(A_K)$  have disjoint supports given by the row/column indices of the blocks.

The following lemma is an immediate consequence of Lemma A.1.

**Lemma A.2.** Let  $\Omega \in \mathcal{M}^p$ . Consider  $B$  and  $\delta$  according to Lemma A.1 and let

$$\gamma := r(B), \quad \sigma_j := \lambda_j(B/\gamma), \quad j = 1, \dots, p, \quad \varepsilon := \delta - \gamma.$$

Then,  $v \in \mathbb{R}^p$  is an eigenvector of  $\Omega$  if and only if it is an eigenvector of  $B$ , and the spectrum of  $\Omega$  is given by  $\lambda_j(\Omega) = \varepsilon + \gamma(1 - \sigma_{p-j+1}) > 0$ ,  $j = 1, \dots, p$ .

*Proof of Theorem 1.* It will be shown that under the stated conditions, there exists  $R < \infty$  such that

$$\min_{\Omega \in \overline{\mathcal{M}^p}} -\log \det(\Omega) + \text{tr}(\Omega S) = \min_{\Omega \in \overline{\mathcal{M}^p}: \|\Omega\| \leq R} -\log \det(\Omega) + \text{tr}(\Omega S), \quad (\text{A.1})$$

which implies existence of a minimizer. Uniqueness readily follows from existence in view of the strict convexity of the negativ log-determinant on  $\overline{\mathbb{S}_+^p}$ . To establish (A.1), it suffices to show that the objective is bounded from below. Let  $\Omega \in \mathcal{M}^p$  be arbitrary. Expanding  $\Omega = \sum_{j=1}^p \lambda_j u_j u_j^\top$ , where  $\lambda_j := \lambda_j(\Omega)$ ,  $j = 1, \dots, p$ , and  $\{u_j\}_{j=1}^p$  are the corresponding eigenvectors, the objective evaluated at  $\Omega$  can be written as

$$\begin{aligned} -\log \det(\Omega) + \text{tr}(\Omega S) &= -\sum_{j=1}^p \log(\lambda_j) + \sum_{j=1}^p \lambda_j u_j^\top S u_j \\ &= -\sum_{j=1}^p \log \{\varepsilon + \gamma(1 - \sigma_{p-j+1})\} + \\ &\quad + \sum_{j=1}^p \{\varepsilon + \gamma(1 - \sigma_{p-j+1})\} u_j^\top S u_j, \end{aligned}$$

where the second equality follows from  $\Omega \in \mathcal{M}^p$  and Lemma A.2. We first note that the objective can be unbounded from below only if  $\gamma$  is unbounded and  $\varepsilon$  is bounded from above, respectively. To show the boundedness of  $\varepsilon$ , note that

$$\begin{aligned} &-\sum_{j=1}^p \log \{\varepsilon + \gamma(1 - \sigma_{p-j+1})\} + \sum_{j=1}^p \{\varepsilon + \gamma(1 - \sigma_{p-j+1})\} u_j^\top S u_j \\ &\geq -\sum_{j=1}^p \log \{\varepsilon + \gamma(1 - \sigma_{p-j+1})\} + \sum_{j=1}^p \varepsilon u_j^\top S u_j \\ &\geq -\sum_{j=1}^p \log \{\varepsilon + \gamma(1 - \sigma_{p-j+1})\} + \varepsilon \max_{1 \leq j \leq p} u_j^\top S u_j. \end{aligned} \quad (\text{A.2})$$

If the objective is unbounded from below,  $\varepsilon$  can hence be unbounded only if  $Su_j = 0$ ,  $j = 1, \dots, p$ , because the first term decreases logarithmically in  $\varepsilon$ , whereas the second term increases linearly in  $\varepsilon$ . The condition  $Su_j = 0$ ,  $j = 1, \dots, p$ , however, implies that  $S$  is the zero matrix, which contradicts the assumption that  $S$  has positive diagonal entries. Using a similar argument as in (A.2) while noting that  $|\sigma_k| \leq 1$ ,  $k = 1, \dots, p$ , if  $\gamma$  is unbounded, the objective can be unbounded from below only if

$$\bigwedge_{j=1}^p (Su_j = 0 \vee \gamma(1 - \sigma_{p-j+1}) = 0) \iff \bigwedge_{j=1}^{p-1} (Su_j = 0 \vee \gamma(1 - \sigma_{p-j+1}) = 0),$$

where the equivalence follows from  $\sigma_1 = \lambda_1(B/\gamma) = 1$  according to Lemma A.2 and the Perron-Frobenius Theorem. Consider now the following cases.

*Case 1.* If  $1 - \sigma_{p-j+1} > 0$ ,  $j = 1, \dots, p-1$ , we must have  $Su_j = 0$ ,  $j = 1, \dots, p-1$ , which implies that  $S$  has rank one.

*Case 2.* If  $1 - \sigma_k = 0$  for some  $k \in \{2, \dots, p\}$ , we have  $\sigma_k = \sigma_1 = r(B)$ . Consequently, the eigenvalue  $\sigma_1$  of  $B$  has multiplicity greater than 1. According to Theorem A.1, the symmetric non-negative matrix  $B$  must be reducible, as must be  $\Omega$ . As a result, there exists a partitioning  $I_1, \dots, I_K$  ( $K \geq 2$ ) of  $\{1, \dots, p\}$  and a permutation matrix  $\Pi$  so that  $\Pi\Omega\Pi^\top = \text{bdiag}(\Omega_{11}, \dots, \Omega_{KK})$ , where  $\Omega_{kk}$  is the principal submatrix corresponding to index set  $I_k$ ,  $k = 1, \dots, K$ . We may assume that the  $\{\Omega_{kk}\}_{k=1}^K$  are irreducible; otherwise, we could simply apply additional permutations to end up with  $K' > K$  blocks that are irreducible. The objective can now be decoupled as follows.

$$\begin{aligned} -\log \det(\Omega) + \text{tr}(\Omega S) &= -\log \det(\Pi\Omega\Pi^\top) + \text{tr}\{(\Pi\Omega\Pi^\top)(\Pi S\Pi^\top)\} \\ &= \sum_{k=1}^K -\log \det(\Omega_{kk}) + \text{tr}(\Omega_{kk} S_{kk}), \end{aligned}$$

where  $S_{kk}$ ,  $k = 1, \dots, K$ , are the principal submatrices of  $\Pi S\Pi^\top$  corresponding to  $\Omega_{kk}$ ,  $k = 1, \dots, K$ . From the last display, we conclude that the objective is unbounded from below only if there exists  $k \in \{1, \dots, K\}$  such that  $-\log \det(\Omega_{kk}) + \text{tr}(\Omega_{kk} S_{kk})$  is unbounded from below. At this point, for each  $k = 1, \dots, K$ , we may recur to the reasoning that has led us to the case distinction above. As the  $\{\Omega_{kk}\}_{k=1}^K$  are irreducible, the second case cannot occur any longer. Consequently, the objective is unbounded from below only if one of the  $\{S_{kk}\}_{k=1}^K$  has rank one, i.e. for some  $k \in \{1, \dots, K\}$ ,

we have that  $S_{kk} = vv^\top$  with  $v \in \mathbb{R}^{|I_k|}$ . Note that if  $|I_k| = 1$ ,  $S_{kk}$  is a scalar, i.e. a diagonal entry of  $S$  which is assumed to be positive, so that  $-\log \det(\Omega_{kk}) + \text{tr}(\Omega_{kk}S_{kk})$  cannot be unbounded from below. If  $|I_k| \geq 3$ , there must exist  $\ell, m \in \{1, \dots, |I_k|\}$ ,  $\ell \neq m$ , so that

$$0 < (S_{kk})_{\ell m} = v_\ell v_m = \sqrt{v_\ell^2 v_m^2} = \sqrt{(S_{kk})_{\ell\ell}(S_{kk})_{mm}}.$$

This can be seen by enumerating all possible sign patterns of  $v$  for  $|I_k| = 3$ , i.e. schematically  $(+, +, +), (-, +, +), \dots, (-, -, +), (-, -, -)$  (note that all entries of  $v$  must be non-zero, since the diagonal entries of  $S$  are positive by assumption) and verifying that at least one of  $v_1 \cdot v_2, v_1 \cdot v_3, v_2 \cdot v_3$  must be positive. To finish the proof of the theorem, it remains to consider the case  $|I_k| = 2$ , where

$$S_{kk} = \begin{pmatrix} v_1^2 & v_1 v_2 \\ v_1 v_2 & v_2^2 \end{pmatrix}.$$

Denote the eigenvectors of  $\Omega_{kk} = \delta_{kk}I - B_{kk}$ , say, by  $z_1$  and  $z_2$ ,  $z_1^\top z_2 = 0$ . Invoking Theorem A.1, we may choose  $z_1$  such that its two entries are of the same sign and those of  $z_2$  have a different sign. Note that since Case 1 (see above) occurs for  $S_{kk}$ , the eigenvector  $z_2$  not corresponding to the largest eigenvalue of  $B$  must satisfy  $S_{kk}z_2 = 0$ . This can hold only if  $v_1 v_2 > 0$ .  $\square$

## Appendix B. Proof of Theorem 2

Let  $\Omega = \Sigma^{-1}$  and consider the Bregman divergence between  $\Omega$  and  $\Omega' \in \overline{\mathbb{S}_+^p}$  which is induced by the log-determinant

$$D(\Omega \parallel \Omega') = -\log \det(\Omega') + \log \det(\Omega) + \text{tr}(\Sigma(\Omega' - \Omega)).$$

In virtue of properties of Bregman divergences, we have

$$D(\Omega \parallel \Omega') \geq 0, \text{ with equality holding if and only if } \Omega' = \Omega. \quad (\text{B.1})$$

If  $\Sigma \in \mathbb{S}_+^p$  is an inverse  $M$ -matrix, then  $\Omega \in \mathcal{M}^p$ . By (B.1) and the definition of  $D$

$$\Omega \in \mathcal{M}^p \implies \Omega = \underset{\Omega' \in \mathcal{M}^p}{\text{argmin}} D(\Omega \parallel \Omega') \iff \Omega = \underset{\Omega' \in \mathcal{M}^p}{\text{argmin}} -\log \det(\Omega') + \text{tr}(\Sigma\Omega').$$

From the duality relation (10), the last property implies that

$$\Sigma = \underset{\Sigma' \in \overline{\mathbb{S}_+^p}, \Sigma' \geq \Sigma, \text{diag}(\Sigma') = \text{diag}(\Sigma)}{\text{argmax}} \log \det(\Sigma') + p$$

For the opposite direction, suppose that  $\Omega \in \mathbb{S}_+^p \setminus \mathcal{M}^p$  and denote  $\Omega_\bullet = \operatorname{argmin}_{\Omega' \in \overline{\mathcal{M}^p}} D(\Omega \parallel \Omega')$ . From (B.1), we have  $D(\Omega \parallel \Omega_\bullet) > 0$  and hence also

$$-\log \det(\Omega_\bullet) + \operatorname{tr}(\Sigma \Omega_\bullet) > -\log \det(\Omega) + \operatorname{tr}(\Sigma \Omega) = \log \det(\Sigma) + p.$$

Denote  $\Sigma_\bullet = \Omega_\bullet^{-1}$ . By definition of  $\Omega_\bullet$  and (10),

$$\log \det(\Sigma_\bullet) + p = -\log \det(\Omega_\bullet) + \operatorname{tr}(\Sigma \Omega_\bullet) > -\log \det(\Omega) + \operatorname{tr}(\Sigma \Omega) = \log \det(\Sigma) + p.$$

It follows that  $\log \det(\Sigma_\bullet) > \log \det(\Sigma)$  with  $\Sigma_\bullet \geq \Sigma$  and  $\operatorname{diag}(\Sigma_\bullet) = \operatorname{diag}(\Sigma)$ .

### Appendix C. Proofs for the Examples in Section 2.3

(3) *AR(2)-structure.* First note that under the condition  $4|\phi_2| < \phi_1$ , it holds that  $\phi_1 > 0$ . Hence if  $\phi_2$  is also non-negative, the parameters of the corresponding AR(2) process and thus all partial correlations are non-negative [45] so that  $\Omega_* \in \mathcal{M}^p$ , in which case property (17) is trivially satisfied. On the other hand, if  $\phi_2 < 0$  while  $4|\phi_2| < \phi_1$ , the sequence  $(\rho_\ell)$  as given in (18) is monotonically decreasing (cf. [10], p.45). This property will allow us to show that  $\Omega_\bullet$  (13) is an  $M$ -matrix corresponding to an AR(1)-structure. To this end, it is established that the inverse  $\Sigma_\bullet$  has entries  $\sigma_{jk}^\bullet = \rho_{|j-k|}^\bullet$ ,  $j, k = 1, \dots, p$ , where with  $\rho_1$  as in (18),

$$\rho_\ell^\bullet = \rho_1^\ell = \left( \frac{\phi_1}{1 - \phi_2} \right)^\ell, \quad \ell = 1, \dots, p - 1.$$

In order to verify the optimality conditions of (13)/(15) according to (8), it suffices to show complementarity slackness (9), that is  $\rho_1^\bullet = \rho_1$  and further  $\rho_\ell^\bullet > \rho_\ell$  for  $\ell = 2, \dots, p - 1$ . The first claim is immediate from (18). The second claim is proved by induction. The base case ( $\ell = 2$ ) follows from

$$\begin{aligned} \rho_2 &= \phi_1 \rho_1 + \phi_2 \\ &= \rho_1(1 - \phi_2) \rho_1 + \phi_2 = \rho_1^2 + \phi_2(1 - \rho_1^2) < \rho_1^2 = \rho_2^\bullet, \end{aligned}$$

since  $\phi_2 < 0$ . Considering  $\ell \geq 3$ , we have

$$\begin{aligned} \rho_\ell &= \phi_1 \rho_{\ell-1} + \phi_2 \rho_{\ell-2} \\ &= \rho_1(1 - \phi_2) \rho_{\ell-1} + \phi_2 \rho_{\ell-2} \\ &= \rho_1 \rho_{\ell-1} + \phi_2(\rho_{\ell-2} - \rho_1 \rho_{\ell-1}) \end{aligned}$$

The second term is negative, because the term inside the brackets is positive, as  $\rho_{\ell-2} > \rho_{\ell-1}$ , recalling that  $(\rho_\ell)$  is monotonically decreasing. By the induction hypothesis,  $\rho_{\ell-1} < \rho_{\ell-1}^\bullet = \rho_1^{\ell-1}$  so that  $\rho_1 \rho_{\ell-1} < \rho_1^\ell$  and consequently  $\rho_\ell < \rho_1^\ell = \rho_\ell^\bullet$ ,  $\ell = 2, \dots, p-1$ , as claimed.  $\square$

(4) *Star structure.* We verify the expressions for  $\Omega_\bullet$  and  $\Sigma_\bullet$  as given in the main text. This is done by checking the KKT optimality conditions of (13), cf.(8). We set

$$\Gamma_\bullet = \begin{pmatrix} 0 & \delta^\top \\ \delta & -\rho\tilde{\rho}^\top - \tilde{\rho}\rho^\top + 2\tilde{\rho}\tilde{\rho}^\top \end{pmatrix},$$

with  $\rho, \tilde{\rho}$  as defined in the main text and  $\delta = \rho - \tilde{\rho}$ , so that  $\Sigma_\bullet = \Sigma_* + \Gamma_\bullet$ . Because of dual feasibility and complementarity slackness, the following has to hold for the entries  $(\gamma_{jk}^\bullet)$  of  $\Gamma_\bullet$ :

- (1) :  $\gamma_{jj}^\bullet = 0$ ,  $j = 1, \dots, p$ ,
- (2) :  $\gamma_{j1}^\bullet = \gamma_{1j}^\bullet = 0$  for all  $j \neq 1$  such that  $\omega_{j1}^\bullet < 0$ ,
- (3) :  $\gamma_{j1}^\bullet = \gamma_{1j}^\bullet > 0$  for all  $j \neq 1$  such that  $\omega_{j1}^\bullet = 0$ ,
- (4) :  $\gamma_{jk}^\bullet = 0$  for all  $(j, k), j, k \neq 1$ , and  $\omega_{jk}^\bullet < 0$ ,
- (5) :  $\gamma_{jk}^\bullet > 0$  for all  $(j, k), j, k \neq 1$ , and  $\omega_{jk}^\bullet = 0$ .

The requirements (2) and (3) follow immediately from the definition of  $\delta$  and  $\tilde{\rho}$ . For the remainder, let  $j, k > 1$  be arbitrary and set  $\ell = j - 1$ ,  $m = k - 1$ . We have that

$$\gamma_{jk}^\bullet = -\rho_\ell \tilde{\rho}_m - \tilde{\rho}_\ell \rho_m + 2\tilde{\rho}_\ell \tilde{\rho}_m \begin{cases} = 0 & \rho_\ell < 0, \rho_m < 0, \\ > 0 & \rho_\ell > 0, \rho_m < 0, \\ > 0 & \rho_\ell < 0, \rho_m > 0, \\ = 0 & \rho_\ell > 0, \rho_m > 0, \\ = 0 & \rho_\ell = 0 \text{ or } \rho_m = 0. \end{cases}$$

The diagonal entries  $\gamma_{jj}^\bullet, j > 1$ , equal zero since for  $\ell = m$ ,  $\rho_\ell = \rho_m$  and consequently  $\text{sign}(\rho_\ell) = \text{sign}(\rho_m)$ , which confirms (1). Concerning (4), note that for  $j \neq k$ ,  $\omega_{jk}^\bullet < 0$  if and only if  $\delta_\ell = \rho_\ell - \tilde{\rho}_\ell > 0$  and  $\delta_m = \rho_m - \tilde{\rho}_m > 0$  if and only if  $\rho_\ell > 0$  and  $\rho_m > 0$  so that the corresponding  $\gamma_{jk}^\bullet = 0$ . Point (5) follows with the converse argument, starting from  $\omega_{jk}^\bullet = 0$  if and only if  $\delta_\ell = 0$  or  $\delta_m = 0$ . We now check the stationarity condition  $\Omega_\bullet = (\Sigma_* + \Gamma_\bullet)^{-1}$ .



We first verify the expression  $I - \delta\delta^\top/(1 + \|\delta\|_2^2)$  for the bottom right block of  $\Omega_\bullet$ . Using Schur complements, we get that the block is given by

$$\begin{aligned} (I + \rho\rho^\top - \rho\tilde{\rho}^\top - \tilde{\rho}\rho^\top + 2\tilde{\rho}\tilde{\rho}^\top - \tilde{\rho}\tilde{\rho}^\top)^{-1} &= (I + (\rho - \tilde{\rho})(\rho - \tilde{\rho})^\top)^{-1} \\ &= (I + \delta\delta^\top)^{-1} = I - \frac{\delta\delta^\top}{1 + \|\delta\|_2^2} \end{aligned}$$

by the Sherman-Woodbury-Morrison formula. For the remaining blocks, one verifies that  $\Omega_\bullet\Sigma_\bullet = I$  directly with matrix multiplication, noting that

$$\tilde{\rho} - (\tilde{\rho} - \delta\delta^\top\tilde{\rho}/(1 + \|\delta\|_2^2)) = 0,$$

because  $\delta^\top\tilde{\rho} = 0$ . To conclude the proof, it remains to check that  $\Omega_\bullet \succ 0$ . We show that all principal minors of  $\Omega_\bullet$  are positive, which requires the following conditions to hold:

$$I - \frac{\delta\delta^\top}{1 + \|\delta\|_2^2} \succ 0, \text{ and } (1 + \|\tilde{\rho}\|_2^2 - \tilde{\rho}^\top(I - \delta\delta^\top/(1 + \|\delta\|_2^2))^{-1}\tilde{\rho}) > 0.$$

The first part follows by noting that the smallest eigenvalue of the matrix is given by  $1 - \|\delta\|_2^2/(1 + \|\delta\|_2^2) > 0$ . The second part results from  $\delta^\top\tilde{\rho} = 0$ .  $\square$

#### Appendix D. Proof of Theorem 3

It is not hard to verify that the conditions of Proposition 2.7.1 in [6], a general result concerning convergence of block coordinate descent, are satisfied. In particular, as discussed in Section 4, the problems associated with each coordinate block are strictly convex and hence have a unique minimizer. Proposition 2.7.1 in [6] then yields that each limit point of the sequence of iterates  $\{\Omega^t\}$  is a stationary point and thus the unique minimizer  $\hat{\Omega}$ . Existence of a limit point requires the  $\{\Omega^t\}$  be contained in a compact set. This follows from

$$\lim_{\|\Omega\| \rightarrow \infty} -\log \det(\Omega) + \text{tr}(\Omega S) = +\infty,$$

which can be established using the reasoning leading to the proof of Theorem 1, and the fact that for all  $t$

$$-\log \det(\Omega^{t+1}) + \text{tr}(\Omega^{t+1}S) \leq -\log \det(\Omega^t) + \text{tr}(\Omega^t S).$$

## Appendix E. Proof of Proposition 1

The proof will be reduced to a general scheme for establishing consistency of  $M$ -estimators. An  $M$ -estimator is defined as maximizer  $\widehat{\theta}$  of a function of the form

$$\theta \mapsto M_n(\theta) := \frac{1}{n} \sum_{i=1}^n m_\theta(X_i),$$

over some metric space  $(\Theta, d)$ , where the random variables  $\{X_i\}_{i=1}^n$  represent the samples drawn i.i.d. according to a certain probability measure.

**Theorem E.1.** *[from Theorem 5.14 in [52]] Let the following conditions be fulfilled.*

1. *The map  $\theta \mapsto m_\theta(x)$  is upper-semicontinuous for almost all  $x$ .*
2. *For every ball  $U \subset \Theta$ ,  $\mathbf{E}[\sup_{\theta \in U} m_\theta(X)] < \infty$ .*
3. *There exists a compact set  $K \subset \Theta$  so that  $\mathbf{P}(\widehat{\theta} \in K) \rightarrow 1$  as  $n \rightarrow \infty$ .*

*Then:  $d(\widehat{\theta}, \Theta_\bullet) \rightarrow 0$  as  $n \rightarrow \infty$ , where  $\Theta_\bullet = \operatorname{argmax}_{\theta \in \Theta} \mathbf{E}[m_\theta(X)]$ .*

Before applying the above theorem, we first state and prove the following lemma.

**Lemma E.1.** *If the random vector  $X$  has finite fourth moments, that is  $\mathbf{E}[X_j^4] < \infty$  for all  $j = 1, \dots, p$ , then the spectrum of the sample covariance matrix  $S = \frac{1}{n} \sum_{i=1}^n (x_i - \mu_*)(x_i - \mu_*)^\top$  satisfies*

$$\lambda_j(S) = \lambda_j(\Sigma_*) + o_{\mathbf{P}}(1), \quad j = 1, \dots, p,$$

*as  $n \rightarrow \infty$  (and  $p$  stays fixed).*

*Proof.* The assumption of having finite fourth moments implies that  $s_{jk} = \sigma_{jk}^* + o_{\mathbf{P}}(1) \forall (j, k)$  and hence also that

$$\|S - \Sigma_*\|_F \leq p^{1/2} \max_{(j,k)} |s_{jk} - \sigma_{jk}^*| = o_{\mathbf{P}}(1).$$

The claim then follows from the Hoffmann-Wielandt Theorem. □

*Proof of Proposition 1.* First note that the sign-constrained log-determinant divergence minimization (6) falls under the framework of M-estimation with  $\Theta = \overline{\mathcal{M}^p}$ ,  $\hat{\theta} = \hat{\Omega}$ , and we may take  $d$  as the metric that is induced by the spectral norm. For the function  $m_\theta$ , we have  $m_\theta(X) = \log \det(\theta) - \text{tr}(\theta X X^\top)$ . We now verify all three conditions of Theorem E.1. The first condition obviously holds true. Regarding 2., let  $U = \{\theta \in \Theta : \|\theta - \theta_0\| \leq r\}$  for some  $\theta_0 \in \Theta$  a ball of radius  $r > 0$ , where  $\|\cdot\|$  denotes the spectral norm. We have

$$\mathbf{E} \left[ \sup_{\theta \in U} \log \det(\theta) - \text{tr}(\theta X X^\top) \right] \leq \sup_{\theta \in U} \log \det(\theta) < \infty,$$

since  $\mathbf{E}[\text{tr}(\theta X X^\top)] \geq 0$  in view of  $\theta \in \overline{\mathbb{S}_+^p}$ , and the first term is bounded from above, because so is  $\sup_{\theta \in U} \|\theta\|$ . We finally turn to 3. Using an eigen-expansion of  $\hat{\Omega}$ , we have

$$\begin{aligned} \log \det(\hat{\Omega}) - \text{tr}(\hat{\Omega} S) &\leq p \log(\lambda_1(\hat{\Omega})) - \lambda_1(\hat{\Omega}) \lambda_p(S) \\ &\leq \underbrace{p \log(\lambda_1(\hat{\Omega})) - \lambda_1(\hat{\Omega}) \{\lambda_p(\Sigma_*)\}}_{=: U(\lambda_1(\hat{\Omega}))} + o_{\mathbf{P}}(1), \end{aligned}$$

using Lemma E.1. On the other hand, since  $\hat{\Omega}$  is a minimizer and  $\Omega_\bullet$  (13) is feasible,

$$\begin{aligned} \log \det(\hat{\Omega}) - \text{tr}(\hat{\Omega} S) &\geq \log \det(\Omega_\bullet) - \text{tr}(\Omega_\bullet S) \\ &\geq p \log(\lambda_p(\Omega_\bullet)) - \lambda_1(S) \sum_{j=1}^p \lambda_j(\Omega_\bullet) \\ &= \underbrace{p \log(\lambda_p(\Omega_\bullet)) - \lambda_1(\Sigma_*) \sum_{j=1}^p \lambda_j(\Omega_\bullet)}_{=: L} + o_{\mathbf{P}}(1) \end{aligned}$$

Therefore, with probability tending to one as  $n \rightarrow \infty$ ,  $\hat{\Omega}$  is contained in the compact set

$$K = \{\Omega : \|\Omega\| \leq B(U, L)\}, \quad \text{where } B(U, L) = \sup\{b \geq 0 : U(b) \geq L\}.$$

Note that  $b$  must be bounded from above as  $\lim_{b \rightarrow \infty} U(b) = -\infty$ .  $\square$

## Appendix F. Proof of Proposition 2

Our proof depends on the following lemma.

**Lemma F.1.** *Consider the system of linear equations  $Ax = b$ , where  $A \in \mathbb{R}_+^{d \times d}$ ,  $x \in \mathbb{R}_+^d$  and  $b \in \mathbb{R}_+^d$  have only non-negative entries. Then  $x_j \leq b_j/a_{jj}$  for all  $j = 1, \dots, d$ .*

*Proof.* For any  $j \in \{1, \dots, d\}$ , we have that  $a_{jj}x_j \leq \sum_{k=1}^d a_{jk}x_k = b_j$ , using the non-negativity of all entries.  $\square$

*Proof of Proposition 2.* We first prove that  $\max_{(j,k) \notin \mathcal{E}^*, j \neq k} (-\widehat{\omega}_{jk}) \leq c_1 B$ . From the KKT optimality conditions (8), we have that  $\widehat{\Sigma} = S + \widehat{\Gamma}$  with  $\widehat{\gamma}_{jj} = 0$  for all  $j$  and  $\widehat{\gamma}_{jk} = 0$  whenever

$$(j, k) \in \widehat{\mathcal{E}}, \quad \text{where } \widehat{\mathcal{E}} = \{(j, k) : \widehat{\omega}_{jk} < 0\},$$

and consequently

$$(j, k) \in \widehat{\mathcal{E}} \implies \widehat{\sigma}_{jk} = s_{jk}. \quad (\text{F.1})$$

Now choose  $(\bar{j}, \bar{k}) \in \Delta = \widehat{\mathcal{E}} \setminus \mathcal{E}^*$  (if  $\Delta = \emptyset$ , the claim would follow trivially) such that

$$\widehat{\omega}_{\bar{j}\bar{k}} = \min_{(j,k) \in \Delta} \widehat{\omega}_{jk}.$$

Using the partitioning scheme (3) with  $\widehat{\Sigma}$  respectively  $\widehat{\Omega}$  and  $j = \bar{j}$ , and using Schur complements, we obtain that

$$\widehat{\sigma}_{\bar{j}} = \frac{\widehat{\Omega}_{\bar{j}\bar{j}}^{-1} (-\widehat{\omega}_{\bar{j}})}{\widehat{\omega}_{\bar{j}\bar{j}} - \widehat{\omega}_{\bar{j}}^\top \widehat{\Omega}_{\bar{j}\bar{j}}^{-1} \widehat{\omega}_{\bar{j}}} = \widehat{\sigma}_{\bar{j}\bar{j}} \widehat{\Omega}_{\bar{j}\bar{j}}^{-1} (-\widehat{\omega}_{\bar{j}}) = s_{\bar{j}\bar{j}} \widehat{\Omega}_{\bar{j}\bar{j}}^{-1} (-\widehat{\omega}_{\bar{j}}). \quad (\text{F.2})$$

Using Schur complements again,

$$\widehat{\Omega}_{\bar{j}\bar{j}}^{-1} = \widehat{\Sigma}_{\bar{j}\bar{j}} - \frac{\widehat{\sigma}_{\bar{j}} \widehat{\sigma}_{\bar{j}}^\top}{\widehat{\sigma}_{\bar{j}\bar{j}}} = \widehat{\Sigma}_{\bar{j}\bar{j}} - \frac{\widehat{\sigma}_{\bar{j}} \widehat{\sigma}_{\bar{j}}^\top}{s_{\bar{j}\bar{j}}} \quad (\text{F.3})$$

Combining (F.2) and (F.3), we obtain

$$\underbrace{\left( \widehat{\Sigma}_{\bar{j}\bar{j}} - \frac{\widehat{\sigma}_{\bar{j}} \widehat{\sigma}_{\bar{j}}^\top}{\widehat{\sigma}_{\bar{j}\bar{j}}} \right)}_{=:\widehat{\Sigma}_{\bar{j}\bar{j}}} (-\widehat{\omega}_{\bar{j}}) = \frac{\widehat{\sigma}_{\bar{j}}}{s_{\bar{j}\bar{j}}}. \quad (\text{F.4})$$

Let  $\mathcal{A}_{\bar{j}} = \{l \in \{1, \dots, p-1\} : (-\widehat{\omega}_{\bar{j}})_l > 0\}$ . Then, (F.4) can equivalently be written as

$$\begin{aligned} \left(\widetilde{\Sigma}_{\bar{j}\bar{j}}\right)_{\mathcal{A}_{\bar{j}}\mathcal{A}_{\bar{j}}}(-\widehat{\omega}_{\bar{j}})_{\mathcal{A}_{\bar{j}}} &= \left(\frac{s_{\bar{j}}}{s_{\bar{j}\bar{j}}}\right)_{\mathcal{A}_{\bar{j}}}, \\ \left(\widetilde{\Sigma}_{\bar{j}\bar{j}}\right)_{\mathcal{A}_{\bar{j}}^c\mathcal{A}_{\bar{j}}}(-\widehat{\omega}_{\bar{j}})_{\mathcal{A}_{\bar{j}}} &= \left(\frac{s_{\bar{j}} + \gamma_{\bar{j}}}{s_{\bar{j}\bar{j}}}\right)_{\mathcal{A}_{\bar{j}}^c}, \end{aligned} \quad (\text{F.5})$$

where we have used (F.1). In order to upper bound  $(-\widehat{\omega}_{\bar{j}k})$ , we consider (F.5). Since  $\widehat{\Omega}_{\bar{j}\bar{j}}$  is an  $M$ -matrix, its inverse  $\widetilde{\Sigma}_{\bar{j}\bar{j}}$  has only non-negative entries, and we are hence in position to apply Lemma F.1. We obtain

$$(-\widehat{\omega}_{\bar{j}k}) \leq \frac{s_{\bar{j}k}/s_{\bar{j}\bar{j}}}{\widehat{\sigma}_{k\bar{k}} - \widehat{\sigma}_{\bar{j}k}^2/\widehat{\sigma}_{\bar{j}\bar{j}}} = \frac{s_{\bar{j}k}/s_{\bar{j}\bar{j}}}{s_{k\bar{k}} - s_{\bar{j}k}^2/s_{\bar{j}\bar{j}}},$$

where the second equality is again a consequence of (F.1). Using that  $\sigma_{\bar{j}k}^* = 0$ ,  $\sigma_{\bar{j}\bar{j}}^* = \sigma_{k\bar{k}}^* = 1$ , the bound (23) yields

$$(-\widehat{\omega}_{\bar{j}k}) \leq \frac{s_{\bar{j}k}}{s_{\bar{j}\bar{j}}s_{k\bar{k}} - s_{\bar{j}k}^2} \leq \frac{B}{1 - 2B - B^2} \leq C_0B \text{ as } n \rightarrow \infty, \quad (\text{F.6})$$

since  $B = o_{\mathbf{P}}(1)$  as  $n \rightarrow \infty$ . In the sequel, we derive a lower bound on the entry of  $(-\widehat{\omega}_{12})$  corresponding to  $\mathcal{E}^*$ . For this purpose, let us re-consider Eq. (F.4) for  $\bar{j} = 1$ , that is  $\widetilde{\Sigma}_{11}(-\widehat{\omega}_1) = \widehat{\sigma}_1/s_{11}$ . Expanding this equation entry-wise, we get

$$\underbrace{\begin{pmatrix} \widetilde{\sigma}_{22} & \widetilde{\sigma}_{23} & \dots & \widetilde{\sigma}_{2p} \\ \widetilde{\sigma}_{23} & \widetilde{\sigma}_{33} & \dots & \widetilde{\sigma}_{3p} \\ \vdots & \vdots & \ddots & \vdots \\ \widetilde{\sigma}_{2p} & \widetilde{\sigma}_{3p} & \dots & \widetilde{\sigma}_{pp} \end{pmatrix}}_{\widetilde{\Sigma}_{11}} \begin{pmatrix} -\widehat{\omega}_{12} \\ -\widehat{\omega}_{13} \\ \vdots \\ -\widehat{\omega}_{1p} \end{pmatrix} = \begin{pmatrix} \widehat{\sigma}_{12}/s_{11} \\ \widehat{\sigma}_{13}/s_{11} \\ \vdots \\ \widehat{\sigma}_{1p}/s_{11} \end{pmatrix},$$

with  $\widetilde{\sigma}_{jk} = \widehat{\sigma}_{jk} - \widehat{\sigma}_{1j}\widehat{\sigma}_{1k}/s_{11}$ ,  $j, k = 2, \dots, p$ . Consider now the top equation

$$\widetilde{\sigma}_{22}(-\widehat{\omega}_{12}) + \underbrace{\sum_{l=3}^p \widetilde{\sigma}_{2l}(-\widehat{\omega}_{1l})}_{=:\delta} = \widehat{\sigma}_{12}/s_{11}. \quad (\text{F.7})$$

The order of the term  $\delta$ , which is the inner product of the first row of  $\tilde{\Sigma}_{11}$  (excluding the diagonal element  $\tilde{\sigma}_{22}$ ) and  $(-\hat{\omega}_{13}, \dots, -\hat{\omega}_{1p})$ , can be upper bounded by taking the corresponding inner products associated with the remaining rows of  $\tilde{\Sigma}_{11}$  as a reference, noting that the  $\{\tilde{\sigma}_{jk}, j \neq k, (j, k) \notin \{1, 2\}\}$  are of the same order, since the  $\{\hat{\sigma}_{jk}, j \neq k, (j, k) \notin \{1, 2\}\}$  are exchangeable. Accordingly, the right hand sides  $\hat{\sigma}_{13}/s_{11}, \dots, \hat{\sigma}_{1p}/s_{11}$  are also of the same order, which is at most  $O_{\mathbf{P}}(B)$  in view of the complementarity slackness condition (F.1) and the scaling of the  $\{s_{jk}/s_{jj}, j \neq k, (j, k) \notin \{1, 2\}\}$  (if  $\hat{\omega}_{13} = \dots = \hat{\omega}_{1p} = 0$ , we would have  $\delta = 0$ ). Formally, the argument reads

$$\begin{aligned} \delta &= \sum_{l=3}^p \tilde{\sigma}_{2l}(-\hat{\omega}_{1l}) \leq C_1 \max_{3 \leq j \leq p} \sum_{l=3}^p \tilde{\sigma}_{jl}(-\hat{\omega}_{1l}) = \max_{3 \leq j \leq p} \hat{\sigma}_{1j}/s_{11} \\ &\leq C_2 \max_{3 \leq j \leq p} s_{1j}/s_{11} \leq C_3 B, \end{aligned} \quad (\text{F.8})$$

as  $n \rightarrow \infty$ . Suppose for a moment that  $(-\hat{\omega}_{12}) > 0$  so that  $\hat{\sigma}_{12} = s_{12}$ . Substituting (F.8) back into (F.7) and resolving for  $(-\hat{\omega}_{12})$ , we obtain

$$\begin{aligned} (-\hat{\omega}_{12}) &= \frac{\hat{\sigma}_{12}/s_{11} - \delta}{\tilde{\sigma}_{22}} = \frac{s_{12}/s_{11} - \delta}{s_{22} - s_{12}^2/s_{11}} \\ &\geq \frac{\rho - C_4 B}{1 - \rho^2 + C_5 B} = (-\omega_{12}^*) - C_6 B, \end{aligned} \quad (\text{F.9})$$

as  $n \rightarrow \infty$ , i.e. if  $\rho > C_4 B$ , we verify that indeed  $(-\hat{\omega}_{12}) > 0$ . Altogether, (F.6) and (F.9) indicate that if  $(-\hat{\omega}_{12}) > t$ ,  $t = (C_0 + C_6)B$ , the thresholding procedure (20) would yield  $\hat{\mathcal{E}}(t) = \mathcal{E}^*$ , i.e. recovery of the edge set.  $\square$

## G. $M$ -matrices and Faithfulness

We show that if the precision matrix of a Gaussian random vector is an  $M$ -matrix, then faithfulness as defined below holds.

**Definition G.1.** [50, 8] *Let  $X$  be a multivariate Gaussian random vector with covariance matrix  $\Sigma \in \mathbb{S}_+^p$ . Then  $X$  is said to have a faithful distribution if for any disjoint triple  $A, B, C$  of subsets of  $\{1, \dots, p\}$ ,*

$$X_A \perp\!\!\!\perp X_B \mid X_C \implies C \text{ separates } A \text{ and } B$$

*in the conditional independence graph associated with  $\Sigma^{-1}$ ,*

*that is, vertices in  $A$  are connected with vertices in  $B$  at most only via vertices in  $C$ .*

Note that the converse statement, i.e. separation of  $A$  and  $B$  by  $C$  in the conditional independence graph implies conditional independence of  $X_A$  and  $X_B$  given  $X_C$ , always holds (global Markov property).

**Proposition G.1.** *If  $\Sigma^{-1} \in \mathcal{M}^p$ , then  $X$  has a faithful distribution.*

*Proof.* In the sequel, we will show that

$$X_A \perp\!\!\!\perp X_B \mid X_C \implies X_A \perp\!\!\!\perp X_B \mid X_{C'} \quad \forall C' \supseteq C, \quad C' \subseteq \{1, \dots, p\} \setminus (A \cup B). \quad (\text{G.1})$$

Choosing  $C' = \{1, \dots, p\} \setminus (A \cup B)$ , the claim follows from the global Markov property w.r.t. the conditional independence graph associated with  $\Sigma^{-1}$ . Let  $\gamma = A \cup B \cup C$ ,  $\gamma' = A \cup B \cup C'$  and  $\Omega^{\gamma\gamma} = \Sigma_{\gamma\gamma}^{-1}$ ,  $\Omega^{\gamma'\gamma'} = \Sigma_{\gamma'\gamma'}^{-1}$ . We will compute  $\Omega^{\gamma'\gamma'}$  incrementally from  $\Omega^{\gamma\gamma}$  by using the decomposition  $C' \setminus C = \{i_1\} \cup \dots \cup \{i_q\}$  ( $q = |C' \setminus C|$ ), successively obtaining  $\Omega^{\gamma_1\gamma_1}, \dots, \Omega^{\gamma_q\gamma_q} = \Omega^{\gamma'\gamma'}$ , where  $\gamma_1 = A \cup B \cup C \cup \{i_1\}, \dots, \gamma_q = A \cup B \cup C \cup \{i_1\} \cup \dots \cup \{i_q\} = \gamma'$ . Starting from  $\Omega^{\gamma_1\gamma_1}$ , we partition its inverse  $\Sigma_{\gamma_1\gamma_1}$  as

$$\Sigma_{\gamma_1\gamma_1} = \begin{pmatrix} \Sigma_{\gamma\gamma} & u_1^\top \\ u_1 & u_{11} \end{pmatrix},$$

where the vector  $u_1$  and the scalar correspond to the added index  $i_1$ . The partitioned inverse formula yields the following for  $\Omega_{\gamma\gamma}^{\gamma_1\gamma_1}$ , the principal submatrix of  $\Omega^{\gamma_1\gamma_1}$  associated with the index set  $\gamma$ :

$$\Omega_{\gamma\gamma}^{\gamma_1\gamma_1} = \left( \Sigma_{\gamma\gamma} - \frac{u_1 u_1^\top}{u_{11}} \right)^{-1} = \Sigma_{\gamma\gamma}^{-1} + \underbrace{\frac{\Sigma_{\gamma\gamma}^{-1} u_1 u_1^\top \Sigma_{\gamma\gamma}^{-1}}{u_{11} - u_1^\top \Sigma_{\gamma\gamma}^{-1} u_1}}_{=: P} = \Omega^{\gamma\gamma} + P,$$

where the second identity results from the Sherman-Woodbury-Morrison formula. Note that  $P$  has only non-negative entries. To verify this, observe that  $\Sigma_{\gamma\gamma}^{-1} u_1$  equals the vector of regression coefficients one obtains when regressing the variable with index  $i_1$  on the variables in  $\gamma$ , which must be non-negative because  $\Sigma^{-1} \in \mathcal{M}^p$  and hence also  $\Sigma_{\gamma_1\gamma_1}^{-1} \in \mathcal{M}^p$  (cf. (12) and the comments thereafter). Furthermore,

$$u_{11} - u_1^\top \Sigma_{\gamma\gamma}^{-1} u_1 = \det(u_{11} - u_1^\top \Sigma_{\gamma\gamma}^{-1} u_1) = \det(\Sigma_{\gamma_1\gamma_1}) / \det(\Sigma_{\gamma\gamma}) > 0$$

in virtue of the positive definiteness of  $\Sigma$ . The non-negativity of  $P$  implies that  $\Omega^{\gamma\gamma} \leq \Omega_{\gamma\gamma}^{\gamma_1\gamma_1}$ . We may now repeat the same argument to obtain successively  $\Omega_{\gamma_1\gamma_1}^{\gamma_2\gamma_2}, \dots, \Omega_{\gamma_{q-1}\gamma_{q-1}}^{\gamma_q\gamma_q}$ . Consequently, we must have  $\Omega^{\gamma\gamma} \leq \Omega_{\gamma\gamma}^{\gamma_q\gamma_q}$  and hence, since  $X_A \perp\!\!\!\perp X_B | X_C$ , in particular that  $0 = \Omega_{AB}^{\gamma\gamma} \leq \Omega_{AB}^{\gamma_q\gamma_q} = \Omega_{AB}^{\gamma'\gamma'}$  (recall that  $\gamma' = A \cup B \cup C'$ ). The inequality must hold with equality, because  $\Omega^{\gamma'\gamma'}$  is a positive definite  $M$ -matrix (cf. (12)). We conclude the assertion from  $\Omega_{AB}^{\gamma'\gamma'} = 0 \iff X_A \perp\!\!\!\perp X_B | X_{C'}$ . □

## References

- [1] A. Anandkumar, V. Tan, F. Huang, and A. Willsky. Supplementary code to 'High-Dimensional Gaussian Graphical Model Selection: Walk-Summability and Local Separation Criterion'. <http://newport.eecs.uci.edu/anandkumar/pubs/GaussianStructLearning-code.zip>.
- [2] A. Anandkumar, V. Tan, F. Huang, and A. Willsky. High-dimensional graphical model selection: Tractable graph families and necessary conditions. *Journal of Machine Learning Research*, 13:2293–2337, 2012.
- [3] O. Banerjee, L. El Ghaoui, and A. d'Aspremont. Model Selection Through Sparse Maximum Likelihood Estimation for Multivariate Gaussian or Binary Data. *Journal of Machine Learning Research*, 9:485–516, 2008.
- [4] A. Berman and R. Plemmons. *Nonnegative matrices in the mathematical sciences*. SIAM Classics in Applied Mathematics, 1994.
- [5] A. Berman and N. Shaked-Monderer. *Completely positive matrices*. World Scientific, 2003.
- [6] D. Bertsekas. *Nonlinear Programming*. Athena Scientific, 1999.
- [7] S. Boyd and L. Vandenberghe. *Convex Optimization*. Cambridge University Press, 2004.
- [8] P. Bühlmann and S. van de Geer. *Statistics for high-dimensional data*. Springer, 2011.



- [9] T. Cai, W. Liu, and X. Luo. A Constrained  $\ell_1$  Minimization Approach to Sparse Precision Matrix Estimation. *Journal of the American Statistical Association*, 106:594–607, 2011.
- [10] C. Chatfield. *The Analysis of Time Series: an introduction*. Chapman & Hall/CRC, 2003.
- [11] S. Chaudhuri, M. Drton, and T. Richardson. Estimation of a covariance matrix with zeros. *Biometrika*, 94:199–216, 2007.
- [12] C. Chow and C. Liu. Approximating discrete probability distributions with dependence trees. *IEEE Transactions on Information Theory*, 14:462–467, 1968.
- [13] T. Cootes. XM2VTS face images. [http://personalpages.manchester.ac.uk/staff/timothy.f.cootes/data/xm2vts/xm2vts\\_markup.html](http://personalpages.manchester.ac.uk/staff/timothy.f.cootes/data/xm2vts/xm2vts_markup.html).
- [14] J. Dahl, V. Roychowdhury, and L. Vandenberghe. Maximum likelihood estimation of Gaussian graphical models: numerical implementation and topology selection. Technical report, University of California, Los Angeles, 2005.
- [15] A. Dempster. Covariance selection. *Biometrics*, 28:157–175, 1972.
- [16] I. Dhillon and J. Tropp. Matrix nearness problems with Bregman divergences. *SIAM Journal on Matrix Analysis and Applications*, 29:1120–1146, 2007.
- [17] I. Dryden and K. Mardia. *Statistical Shape Analysis*. Wiley, 2002.
- [18] J. Duchi, S. Gould, and D. Koller. Projected subgradient methods for learning sparse Gaussians. In *Artificial Intelligence and Statistics (AISTATS)*, 2009.
- [19] E. Bølviken. Probability inequalities for the multivariate normal with non-negative partial correlations. *Scandinavian Journal of Statistics*, 9:49–58, 1982.
- [20] J. Fan, Y. Feng, and Y. Wu. Network exploration via the adaptive lasso and SCAD penalties. *The Annals of Applied Statistics*, 3:521–541, 3.

- [21] R. Foygel and M. Drton. Extended Bayesian information criteria for Gaussian graphical models. In *Advances in Neural Information Processing Systems 23*, pages 2020–2028, 2010.
- [22] J. Friedman, T. Hastie, and R. Tibshirani. Sparse inverse covariance estimation with the graphical lasso. *Biostatistics*, 9:432–441, 2008.
- [23] M. Grant and S. Boyd. CVX: Matlab software for disciplined convex programming, version 1.21, 2011.
- [24] L. Gu, E. Xing, and T. Kanade. Learning GMRF Structures for Spatial Priors. In *CVPR*, 2007.
- [25] J. Honorio, L. Ortiz, and D. Samaras. Sparse and Locally Constant Gaussian Graphical Models. In *Advances in Neural Information Processing Systems 22*. 2009.
- [26] <http://www.mturk.com>.
- [27] M. Kalisch and P. Bühlmann. Estimating High-Dimensional Directed Acyclic Graphs with the PC-Algorithm. *Journal of Machine Learning Research*, 8:613–636, 2007.
- [28] M. Kalisch, M. Mächler, D. Colombo, M. Matthuis, and P. Bühlmann. Causal inference using graphical models with the R package pcalg. *Journal of Statistical Software*, 47:1–26, 2012.
- [29] S. Karlin and Y. Rinott. Classes of orderings of measures and related correlation inequalities I: multivariate totally positive distributions. *Journal of Multivariate Analysis*, 10:467–498, 1980.
- [30] S. Karlin and Y. Rinott. M-matrices as covariance matrices of multinormal distributions. *Linear Algebra and Its Applications*, 52:419–438, 1983.
- [31] H. Karshenas. Graphical lasso in R and MATLAB. <http://www-stat.stanford.edu/~tibs/glasso/>.
- [32] B. Lake and J. Tenenbaum. Discovering Structure by Learning Sparse Graphs. In *Proceedings of the 33rd Annual Cognitive Science Conference*, 2010.

- [33] S. Lauritzen. *Graphical Models*. Oxford University Press, 1996.
- [34] Z. Luo and P. Tseng. On the convergence of the coordinate descent method for convex differentiable minimization. *Journal of Optimization Theory and Applications*, 72:7–35, 1992.
- [35] D. Malioutov, J. Johnson, and A. Willsky. Walk-Sums and Belief Propagation. *Journal of Machine Learning Research*, 7:2031–2064, 2006.
- [36] K. Mardia, J. Kent, and J. Bibby. *Multivariate Analysis*. Academic Press, 1979.
- [37] N. Meinshausen. Sign-constrained least squares estimation for high-dimensional regression. *The Electronic Journal of Statistics*, 7:1607–1631, 2013.
- [38] N. Meinshausen and P. Bühlmann. High-dimensional graphs and variable selection with the lasso. *The Annals of Statistics*, 34:1436–1462, 2006.
- [39] D. Osherson, J. Stern, O. Wilkie, M. Stob, and E. Smith. Default probability. *Cognitive Science*, 15:251–269, 1991.
- [40] A. Ostrowski. Über die Determinanten mit überwiegender Hauptdiagonale. *Commentarii Mathematici Helvetici*, 10:69–96, 1937.
- [41] L. Portugal, J. Judice, and L. Vicente. A comparison of block pivoting and interior-point algorithms for linear least squares problems with non-negative variables. *Mathematics of Computation*, 63:625–643, 1994.
- [42] P. Ravikumar, M. Wainwright, G. Raskutti, and B. Yu. High-dimensional covariance estimation by minimizing  $\ell_1$ -penalized log-determinant divergence. *The Electronic Journal of Statistics*, 4:935–980, 2011.
- [43] Y. Rinott and M. Scarsini. Total positivity order and the normal distribution. *Journal of Multivariate Analysis*, 97:1251–1261, 2004.
- [44] A. Rothman, P. Bickel, L. Levina, and J. Zhu. Sparse permutation invariant covariance estimation. *The Electronic Journal of Statistics*, 2:494–515, 2008.

- [45] H. Rue and L. Held. *Gaussian Markov Random Fields*. Chapman and Hall/CRC, Boca Raton, 2001.
- [46] M. Schmidt. L1General: minimizing differentiable functions with L1-regularization. <http://www.di.ens.fr/~mschmidt/Software/L1General.html>.
- [47] X. Shen, W. Pan, and Y. Zhu. Likelihood-based selection and sharp parameter estimation. *Journal of the American Statistical Association*, 107:223–232, 2012.
- [48] M. Slawski. Problem-specific performance analysis of non-negative least squares solvers with a focus on instances with sparse solutions. Working manuscript, 2013.
- [49] M. Slawski and M. Hein. Sparse recovery by thresholded non-negative least squares. In *Advances in Neural Information Processing Systems 24*, pages 1926–1934. 2011.
- [50] P. Spirtes, C. Glymour, and R. Scheines. *Causation, Prediction, and Search*. MIT press, 2000.
- [51] C. Uhler. Geometry of maximum likelihood estimation in Gaussian graphical models. *The Annals of Statistics*, 40:238–261, 2012.
- [52] A. van der Vaart. *Asymptotic Statistics*. Cambridge University Press, 1998.
- [53] J. Whittaker. *Graphical Models in Applied Multivariate Statistics*. Wiley, Chichester, 1990.
- [54] M. Yuan. High Dimensional Inverse Covariance Matrix Estimation via Linear Programming. *Journal of Machine Learning Research*, 11:2261–2286, 2010.
- [55] M. Yuan and Y. Lin. Model Selection and Estimation in the Gaussian Graphical Model. *Biometrika*, 94:19–35, 2007.
- [56] S. Zhou, P. Rütimann, M. Xu, and P. Bühlmann. High-dimensional covariance estimation based on Gaussian graphical models. *Journal of Machine Learning Research*, 12:2975–3026, 2011.